



Investigation of concrete from Solsvik field station

Etatsprogrammet Varige konstruksjoner 2012-2015

STATENS VEGVESENS RAPPORTER

Nr. 353



Tittel

Undersøkelse av betonger fra Solsvik feltstasjon

Undertittel

4 betongkjerner undersøkt etter 16 års neddykket eksponering

Forfatter

Klaartje De Weerdt, Mette Geiker og Denisa Orsakova

Avdeling

Trafikksikkerhet, miljø- og teknologiavdelingen

Seksjon

Tunnel og betong

Prosjektnummer

603242

Rapportnummer

Nr. 353

Prosjektleder

Synnøve A. Myren / Bård Pedersen

Godkjent av

Claus K. Larsen

Emneord

Slagg, flygeaske, silikastøv, klorid-inntrengning, faseendringer

Sammendrag

Studien har tatt for seg fire av betongene fra Solsvik prøvingsfelt, alle eksponert i 16 år i sjøvann. Betonger med 3 ulike bindemidler ble undersøkt: Portlandsement og 9 % silikastøv, sement med 20 % flygeaske og 4 % silikastøv, og sement med 30 % slagg og 5 % silikastøv, i tillegg til en betong med lettilslag. Hensikten var å undersøke hvordan ulike bindemidler og lettilslag påvirker kloridinntrengning. Det ble fokusert på faseendringer nær betongens overflate og endringer i fuktinnhold. De ulike bindemidlene har gitt omtrent likeverdig kloridinntrengning, mens betong med lettilslag har gitt noe høyere kloridkonsentrasjon nær overflaten men mindre inntrengningsdybde sammenlignet med de øvrige undersøkte betongene. En observasjon fra studien er at betongene ikke er fullt vannmettede på tross av 16 års neddykking.

Title

Investigation of concrete from Solsvik field station

Subtitle

4 concrete cores investigated after 16 years of submerged exposure

Author

Klaartje De Weerdt, Mette Geiker og Denisa Orsakova

Department

Traffic Safety, Environment and Technology Department

Section

Tunnel and concrete

Project number

603242

Report number

No. 353

Project manager

Synnøve A. Myren / Bård Pedersen

Approved by

Claus K. Larsen

Key words

Slag cement, fly ash, silica fume, chloride ingress, phase changes

Summary

Four concretes from the Solsvik field station all submerged in seawater for 16 years have been investigated. Concretes with 3 different binders were included: Portland cement with 9 % SF, cement with 20 % fly Ash and 4 % SF and cement with 30 % slag and 5 % SF. In addition, a concrete containing light weight aggregate was included. The aim of this study was to investigate how different binders and LWA influence the chloride ingress, focusing on phase changes near the concrete surface. The chloride profiles appeared to be relatively similar for the 3 different binders, while the LWA concrete shows higher chloride concentration near the surface and lower ingress depth compared to the other concretes. One remarkable observation is that the centres of the concrete cores are not fully saturated despite 16 years of submersion. Investigation of concrete from Solsvik field station

Forord

Denne rapporten inngår i en serie rapporter fra **etatsprogrammet Varige konstruksjoner**. Programmet hører til under Trafikksikkerhet-, miljø- og teknologiavdelingen i Statens vegvesen, Vegdirektoratet, og foregår i perioden 2012-2015. Hensikten med programmet er å legge til rette for at riktige materialer og produkter brukes på riktig måte i Statens vegvesen sine konstruksjoner, med hovedvekt på bruer og tunneler.

Formålet med programmet er å bidra til mer forutsigbarhet i drift- og vedlikeholdsfasen for konstruksjonene. Dette vil igjen føre til lavere kostnader. Programmet vil også bidra til å øke bevisstheten og kunnskapen om materialer og løsninger, både i Statens vegvesen og i bransjen for øvrig.

For å realisere dette formålet skal programmet bidra til at aktuelle håndbøker i Statens vegvesen oppdateres med tanke på riktig bruk av materialer, sørge for økt kunnskap om miljøpåkjenninger og nedbrytningsmekanismer for bruer og tunneler, og gi konkrete forslag til valg av materialer og løsninger for bruer og tunneler.

Varige konstruksjoner består, i tillegg til et overordnet implementeringsprosjekt, av fire prosjekter:

- Prosjekt 1: Tilstandsutvikling bruer
- Prosjekt 2: Tilstandsutvikling tunneler
- Prosjekt 3: Fremtidens bruer
- Prosjekt 4: Fremtidens tunneler

Varige konstruksjoner ledes av Synnøve A. Myren. Mer informasjon om prosjektet finnes på vegvesen.no/varigekonstruksjoner

Denne rapporten tilhører **Prosjekt 1: Tilstandsutvikling bruer** som ledes av Bård Pedersen. Prosjektet vil generere informasjon om tilstanden for bruer av betong, stål og tre, og gi økt forståelse for de bakenforliggende nedbrytningsmekanismene. Dette vil gi grunnlag for bedre levetidsvurderinger og reparasjonsmetoder. Innenfor områdene hvor det er nødvendig vil det etableres forbedrede rutiner og verktøy for tilstandskontroll- og analyse. Prosjektet vil også frembringe kunnskap om konstruktive konsekvenser av skader, samt konstruktive effekter av forsterkningstiltak. Prosjektet vil gi viktig input i forhold til design av material- og konstruksjonsløsninger for nyere bruer, og vil således ha leveranser av stor betydning til Prosjekt 3: Fremtidige bruer.

Rapporten er utarbeidet av Klaartje De Weerd og Mette Geiker, NTNU, og Denisa Orsakova, Brno Technical University, Tsjekia, som del av et samarbeidsprosjekt mellom NTNU og Varige konstruksjoner.

Data report

Investigation of 4 concrete cores after 16 years of submerged exposure at Solsvik



Date: 14 October 2014

Author: Klaartje De Weerd, Mette Geiker
Norwegian University of Science and Technology
Denisa Orsakova
Brno Technical University, Czech Republic

Sponsor: Statens Vegvesen, Veidirektoratet
PO Boks 8142 Dep
0033 Oslo

Project name: Research and development collaboration agreement between NPRA and NTNU
(FoU samarbeid Varige konstruksjoner TB1 - Kloridinntrengning i betong)

Project no.: SVV: 2012081554, NTNU: 25116700

Preface

The report is prepared as part of a Research and development collaboration agreement between NPRA and NTNU (FoU samarbeid Varige konstruksjoner TB1 - Kloridinntrengning i betong, saksnummer: 2012081554, dated 29.6.2012).

The specific goal of this report is to give an overview of the experimental data obtained from the investigation of concrete cores extracted from the submerged part of 4 concrete beams exposed for 16 years at Solsvik field station.

NRPA's motivation for the collaboration is:

«Statens vegvesen har et stort antall bruer utsatt for meget høy kloridbelastning som følge av plassering langs kysten med værhardt marint klima. Kloridinntrengning inn til armeringen fører til korrosjonskader som nedsetter sikkerheten, øker vedlikeholdskostnadene og forkorter bruens levetid.

Betongbruene i Norge har tradisjonelt vært bygget av betong med ordinære Portlandsementer (CEM I), men fra begynnelsen av 90-tallet alltid i kombinasjon med silikastøv (SV-40 betong). Sementer med flygeaske har i varierende grad vært på markedet fra midten av 80-tallet, og i løpet av de siste årene har flygeaskesementer med 17-20 % flygeaske (klasse CEM II/A-V) blitt dominerende på det norske markedet. Om endringene i betongsammensetning de siste 15-20 årene har hatt den nødvendige effekt er ikke verifisert i særlig grad, og en slik aktivitet er derfor av stor betydning for vurdering av betongbruers levetid i fremtiden.

Betonger med flygeaske og slagg utmerker seg ved å være svært tette og utvikle meget god motstand mot kloridinntrengning, i tillegg utvikler de meget høy elektrisk resistivitet over tid. Det finnes etter hvert en rekke internasjonale erfaringer med både slagg- og flygeaskebetonger, der spesielt de danske erfaringene med flygeaskebetonger er av spesiell interesse»

The overall objective of the collaboration is to improve the basis for selection of binders for reinforced concrete structures in marine exposure. Special focus is placed on how low-carbon binders with high fly ash and slag content resist chloride ingress.

Contents

1	Introduction.....	1
2	Materials.....	3
2.1	Concrete composition of the investigated beams	3
2.2	Extraction of concrete cores and sampling.....	4
3	Experiments.....	6
3.1	Chloride titration	6
3.2	ICP-MS	6
3.3	TGA	6
3.4	SEM-EDS	7
3.5	Microscopy	7
3.6	PF method	7
3.7	RH	8
4	Results	9
4.1	Chloride titration	9
4.2	ICP-MS	11
4.3	TGA	15
4.4	SEM-EDS	19
4.5	Microscopy	26
4.6	PF-method	27
4.7	RH	28
5	Discussion.....	30
6	Conclusion	34
7	Acknowledgements.....	35
8	References.....	35
	Appendix.....	1

1 Introduction

Chloride initiated reinforcement corrosion was in Norway identified and acknowledged as the most severe deteriorating process for marine concrete bridges in the late 1980's. The Norwegian Public Roads Administration (NPRA), as an owner of several hundred large concrete bridges in harsh marine environment and about 12 000 concrete bridges in total, initiated therefore several large research projects focusing on deterioration and durability of reinforced concrete. The main objective for these research projects is to develop concrete types with well documented properties related to deterioration in general and chloride induced reinforcement corrosion in particular. In other words, the best concretes should provide sufficient protection against failure due to reinforcement corrosion in the designated service life, which is 100 years for bridges in Norway. [1]

The Solsvik field station, near Bergen, is one of the three exposure sites which have been established by the NPRA along the Norwegian coast during the '90s. In 1997, concrete beams prepared with 14 different concrete types were exposed at the site.



Figure 1: Lifting a pair of beams at the Solsvik field station for the extraction of cores (2013-08-12).

The reported investigation was made as an in-depth supplementary study of a large investigation done by the NPRA, in which chloride profiles, moisture condition, porosity and electrical resistivity from three different exposure conditions (submerged, tidal and atmospheric) were measured for all 14 concretes.

Of the 14 different concrete compositions three concretes were selected as they have a similar water to binder ratio and cement type, but different binders: Portland cement with silica fume, slag cement and fly ash cement. Ideally a concrete with the same Portland cement but without supplementary cementitious materials (SCMs) such as silica fume, fly ash or slag should have been chosen as a reference, but no such concrete was available. In addition a fourth concrete containing light weight aggregates (Stalite type) and a Portland cement binder was selected. Submerged samples were

selected in an attempt to reduce the ingress mechanisms to mainly diffusion and to eliminate the possible drying and wetting action (except for initial submergence).

From literature it can be seen that supplementary cementitious materials (SCMs) can improve the resistance of concrete to chloride penetration [2]. However, this depends on the type of SCMs used, the replacement level of ordinary Portland cement by the SCMs, the water to binder ratio, and the curing and exposure conditions of the concrete.

The aim of this study was to investigate how the different binders and the LWA influence the chloride ingress, focusing on the phase changes in the concrete near the surface due to long term exposure to sea water, and taking into account the possible changes in the moisture conditions even though the concrete is submerged.

This data report gives an overview of the experimental data obtained from the investigation of the concrete cores extracted from the submerged part of 4 concrete beams exposed for nearly 16 years at Solsvik field station. The data presented in this report is summarized in tables in the Appendix. The authors are currently working on an article which will contain a brief literature review and a more elaborate discussion.

2 Materials

2.1 Concrete composition of the investigated beams

The composition of the concrete of the beams exposed at Solsvik was supplied by the NPRA [3]. Table 1 gives an overview of the information received regarding the concrete composition of the examined beams. Table 2 gives a simplified overview of the binder composition of the investigated concrete beams.

All concrete beams were cast in Oct 1997 at a ready mix concrete plant and stored outdoors (-2 to 10°C) after 1 day for 2 months prior to exposure at the Solsvik field station, except for the OPC-LWA which was cast March 1998 and exposed in July the same year.

Table 1: Concrete composition of the investigated beams [kg/m³ if not indicated differently] [3]

	OPC-SF	OPC-slag	OPC-FA	OPC-LWA
STD cement ¹	2.4	2.6	2.5	
ANL cement	376		336	435
slag cement		391		
fly ash (FA)			84	
silica fume (SF)	34	16	17	25
water	181	165	186	185
absorbed water	15	15	14	
fine aggregate (0-8 mm) ²	872	889	795	738
coarse aggregate (8-16 mm) ³	898	920	926	
light weight aggregate (LWA) ⁴				587
SP (P-stoff)	1.4	1.4	1.4	1.4
SP (HP-SF)	1.1	1.7	1.9	
SP (scanflyt)				1.6
air entrainer	0.12	0.04	0.14	0.5
fresh density	2382	2398	2364	1975
air% -PF	2	2.2	2	
air% - fresh	3	3	3.6	5.2
capillary porosity%	13.2	16.5	14.5	14.9
Paste vol%-ex. Air	31.7	32.7	34	33.5
w/b=free water/c+s+f	0.44	0.40	0.42	0.40
w/c	0.48	0.48	0.55	0.43

⁽¹⁾ Due to the set-up at the ready mix plant a small amount of STD cement needed to be included in the mix. ⁽²⁾ The fine aggregate originates from Holandsfjorden Fonndalen. ⁽³⁾ The coarse aggregate is a glacial fluvial aggregate from Modalen. ⁽⁴⁾ The LWA aggregate is a stalite type.

Table 2: Simplified overview of the binder compositions of the concretes of the investigated beams

	OPC-SF	OPC-slag	OPC-FA	OPC-LWA
ANL cement (CEM I)	X		X	X
Portland slag cement (CEM II/B-S)		X		
fly ash (FA)			20%	
slag		30%		
silica fume (SF)	9%	4%	5%	5%
w/b	0.44	0.40	0.42	0.40

2.2 Extraction of concrete cores and sampling

The extraction of the cores was performed 12 August 2013. Klaartje De Weerd (NTNU, Norway), Mette R Geiker (NTNU, Norway), Denisa Orsakova (BTU, Czech Republic) and Arnaud Muller (EPFL, Switzerland) as well as Bård Pedersen (NPRA, Norway) and Claus K Larsen (NPRA, Norway) were present at Solsvik during the core drilling.

The concrete beams exposed at Solsvik station have a length of 3 m, width of 0.30 m and depth of 0.15 m. The beams are hanging in pairs from the dock and half of the beam is submerged in the sea water. The examined beams are reinforced with a single large stirr-up. For the extraction of the concrete cores the beams were lifted onto the dock by a crane (see Figure 1).

Two cores were extracted from the submerged part of the beams. The cores used for moisture measurements had a diameter of 90 mm and a length of 150 mm, and were taken at approx. 320 mm from the bottom of the beam. The cores used for chemical analysis had a diameter of 75 mm and a length of 150 mm, and were taken at approx. 420 mm from the bottom of the beam. Figure 2 shows the positioning of the extracted cores on the concrete beam.

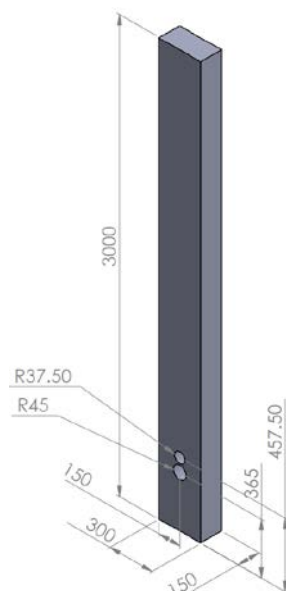


Figure 2: Positioning of the extracted cores in the concrete beam, dimensions given in [mm].

Immediately after extraction the cores were rapidly immersed in a bucket with tap water and dried with a moist cloth to remove slurry from the core drilling. After this the cores were wrapped with plastic foil, put in a plastic bag and sealed with tape. Subsequently they were put in another plastic bag and sealed once more with tape. The cores were subdivided in the laboratory the following day to limit moisture redistribution. The cores were stored at the laboratory temperature prior to testing (approx. 20°C).

Figure 3 shows a sketch of the sample extraction of core used for chemical analysis ($\varnothing 75$ mm). The core was split in two parts along its axis. One half was used for profile grinding in the following sections: 0-1, 1-3, 3-5, 5-7, 7-9, 9-13, 13-17, 17-23, 23-29, 29-35, 35-43, 43-51, 51-59, 59-67, 67-75, 75-83, and 83-91 mm. The powder was collected in sealed plastic bags and stored in a desiccator prior to analysis. The powder was used for TG analysis and was solubilized in acid for chloride titration and ICP-MS. The other half of the cylinder was used for the extraction of fluorescent impregnated polished thin section to be examined with both light microscopy and scanning electron microscopy (SEM).

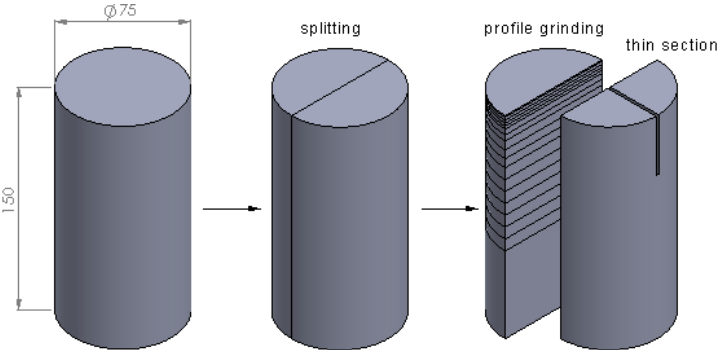


Figure 3: Sketch of the extraction of the samples for chemical and microstructural analysis from the concrete cores [mm].

Figure 4 show a sketch of the sample extraction of the core used for moisture and porosity measurements ($\varnothing 90$ mm). The core was subdivided in the laboratory the day following drilling to limit moisture redistribution. After unwrapping the core, several scales were drawn on the cylindrical surface of the core in order to track the position of the samples during subdivision. The core was split in two. One half is used for porosity and moisture measurements and the other half for relative humidity measurements (RH). The half core was subdivided inwards from the exposed surface into 6 slices each 10 mm thick, approximately over approx. the first 75 mm (6x10 mm + 5x 3 mm lost with cutting). The core was cut into slices using a mechanical saw and water cooling. From the centre of the core some samples were split off.

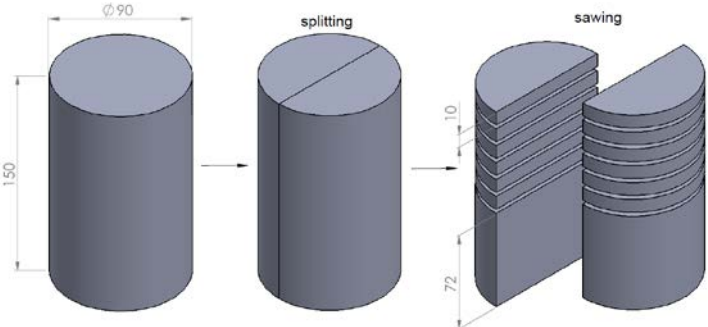


Figure 4: Sketch of the extraction of samples for moisture measurements from the concrete core [mm].

3 Experiments

The relation between the techniques applied and the properties investigated is given in Table 3. In this chapter the methods are described.

Table 3: Schematic overview over the applied methods and the properties investigated

	Chloride ingress	Carbonation	Elemental changes	Porosity	Moisture
Chloride titration	X				
ICP-MS	X		X		
TGA		X			
SEM-EDS	X		X		
Microscopy		X		X	
PF-method				X	X
RH					X

3.1 Chloride titration

About 4 g of the profile ground concrete powder was weighed prior and after drying over night at 105°C in order to determine the moisture content. The dried powder was dissolved in 50 ml 80°C HNO₃(1:10). The suspension was stirred and left to stand for 1 hour. The solution was filtrated with a syringe and a microfilter. Potentiometric titration was performed with a Titrand 905 titrator from Metrohm. The filtrate was loaded in the automatic sampler of the titrator and titrated with 0.01M AgNO₃. The chloride content is expressed relative to the dry mass of the concrete.

3.2 ICP-MS

The filtrate prepared for Cl titration was also analyzed with ICP-MS (inductively-coupled plasma mass spectrometry) to determine the concentration of Al, Ca, Cl, Fe, K, Na, Mg, and S. The concentrations of the different elements measured in the solution are recalculated relative to the dry concrete mass (weight after drying at 105°C).

3.3 TGA

The thermogravimetric analysis (TGA) was performed with a Mettler Toledo TGA/SDTA851, on profile ground powder samples of approximately 300 mg loaded in 900 µl alumina crucibles. The samples were heated up from 40 to 1100°C at a rate of 10°C/min while the oven was purged with N₂ at 50 ml/min. The weight loss of the samples is monitored as a function of the temperature. The weight loss due to the release of bound water (H), decomposition of calcium hydroxide (CH), and release of CO₂ is measured in the respective temperature intervals 40-450°C, 450-550°C, and 550-800°C. The exact limits for the temperature intervals were determined based on the derivative

thermogravimetric curves (DTG). The amount of calcium hydroxide is calculated by multiplying the weight loss with 74/18 (molar mass $\text{Ca}(\text{OH})_2$ / molar mass H_2O).

3.4 SEM-EDS

Polished fluorescence impregnated thin sections were prepared by Pelcon Materials & Testing ApS. The polished sections were investigated with a JEOL JSM-7001F field emission scanning electron microscope combined with a Genesis energy dispersive spectrometer (EDS) operated at an accelerating voltage of 15 kV. EDS elemental maps were obtained by measuring the elemental composition of an area ($125 \times 165 \mu\text{m}$). The elements recorded are Ca, Si, Al, Fe, S, Mg, Cl, Na and K. Aggregates were assumed not to contain Ca. The elemental changes in the cement paste were therefore determined by expressing the results relative to the Ca content. In addition one larger elemental map was made for the OPC-LWA polished thin section to investigate possible binding of chlorides by the LWA.

3.5 Microscopy

The polished thin sections were examined with an Eclipse LV100 POL polarisation microscope from Nikon in order to reveal the spatial distribution of the carbonation and to investigate changes in porosity in the section. It should be noted that the OPC-LWA thin section was not investigated with light microscopy.

3.6 PF method

With the PF method the suction porosity and macro porosity as well as the degree of capillary saturation is determined by weighing samples under different conditions [4, 5]. In this report a slightly altered set-up is used which is described in detail hereunder.

For the porosity and moisture content measurements the concrete discs obtained after sawing were cleaned with a wet cloth. The slices were immediately weighed on a balance with accuracy 0.001 g (W_1). The samples were put into a water bath (partly submerged the first day) until constant mass (mass change over half a day $< 0.01\%$, min 1 week) after which they were weighed in air (W_2) and under water for volume determination ($W_2' = V$). The samples were subsequent put to dry at 50°C until constant mass (W_3^*): approx. 4 weeks. They are then further dried at 105°C until constant mass (W_3): approx. 2 weeks. Then the samples were put into a water bath again (partly submerged the first day) until constant mass (approximately 3 weeks) after which they were weighed in air (W_4) and under water for volume determination ($W_4' = V$). After this the samples were put for 24 hours in a pressure tank at 5 MPa and were weighed immediately after removing the pressure to prevent the loss of water (W_5). Finally the samples were dried at 105°C until constant mass and weighed in air (W_6). The mass W_6 was compared to W_3 and found similar, confirming that the concrete pieces survived the process without damage. Based on the determined masses the following properties of the concrete samples were calculated:

Suction porosity 105°C (capillary and gel porosity)	$(W_2 - W_3)/V$
Suction porosity 50°C (capillary and gel porosity)	$(W_2 - W_3^*)/V$
Air voids or macro porosity	$(W_5 - W_2)/V$
Degree of capillary saturation	$(W_1 - W_3)/(W_2 - W_3)$

3.7 RH

For the relative humidity (RH) measurements, the concrete disc obtained after sawing were cleaned with a wet cloth. The discs were subsequently crushed by hitting them with a hammer while keeping them in a strong plastic bag. The resulting crushed samples were poured over a 2 mm sieve. The finer particles were discarded as they are more subjected to immediate moisture loss. The coarser particles are stored in a glass test tube and sealed with a rubber plug and parafilm®. The test tubes are labelled with the core number and depth of the original concrete disc and stored in a 20°C acclimatized room.

The Vaisala® RH sensors are calibrated over saturated salt solutions (NaCl 75%RH, KCl 85%RH, Na₂SO₄ 93%RH, K₂SO₄ 97%RH at 20°C) prior to measuring the samples. This way a calibration curve for each of the sensors is obtained. When measuring the RH of a sample the RH sensor is inserted in the test tube and sealed with a plug with a cylindrical hole for the cable of the sensor. The RH values are measured manually twice a day until a stable reading is registered (3-7 days).



Figure 5: RH measurements –measuring set-up

4 Results

4.1 Chloride titration

The chloride profiles for the different tested concretes after nearly 16 years of submerged exposure at Solsvik are shown in Figure 6.

There is no large difference between the concretes with the different binders: OPC-SF, OPC-slag and OPC-FA. The surface concentrations (section 0-1 mm) measured do not exhibit the highest chloride concentrations. The profiles all reach a maximum at the 1-3 mm section, and decrease when moving deeper inwards from the exposed surface. Of the concretes with normal weight aggregates tested, the OPC-slag binder performs slightly better than the OPC-SF and OPC-FA binder as it reaches the 0.07% chloride limit, associated with negligible risk of corrosion [6], in the section 23-29 mm whereas the other two reach that limit at 35-43 mm. The fly ash containing concrete (OPC-FA) had a higher maximum chloride content compared to the OPC-slag and OPC-SF concretes.

The OPC-LWA concrete exhibits a wider peak compared to the other concretes, but the chloride content decreases faster after 10 mm. The OPC-LWA concrete reaches the 0.07% chloride content at 29-35 mm.

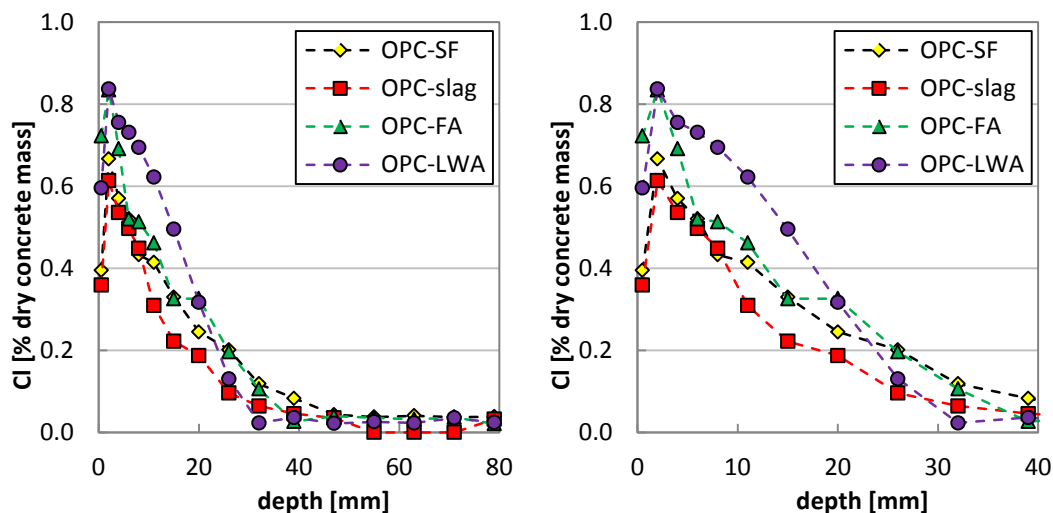


Figure 6: Chloride profiles determined by titration on profile ground cores drilled from the submerged part of the OPC-SF, OPC-slag, OPC-FA and OPC-LWA concrete beams after 16 years of exposure at the Solsvik exposure site. Left: entire tested profile up to 80 mm from the exposed surface; Right: zoomed into the first 40 mm from the exposed surface.

Figure 7 shows the moisture profiles measured on the profile ground powder prior to chloride titration. It should be noted that the powder might have lost moisture during the grinding step. One can however observe that for all the tested cores a relatively constant moisture content from 10-20 mm and inwards, and that there is an increasing trend in the moisture content from 10-20 mm towards the exposed surface. The OPC-FA results are a bit odd.

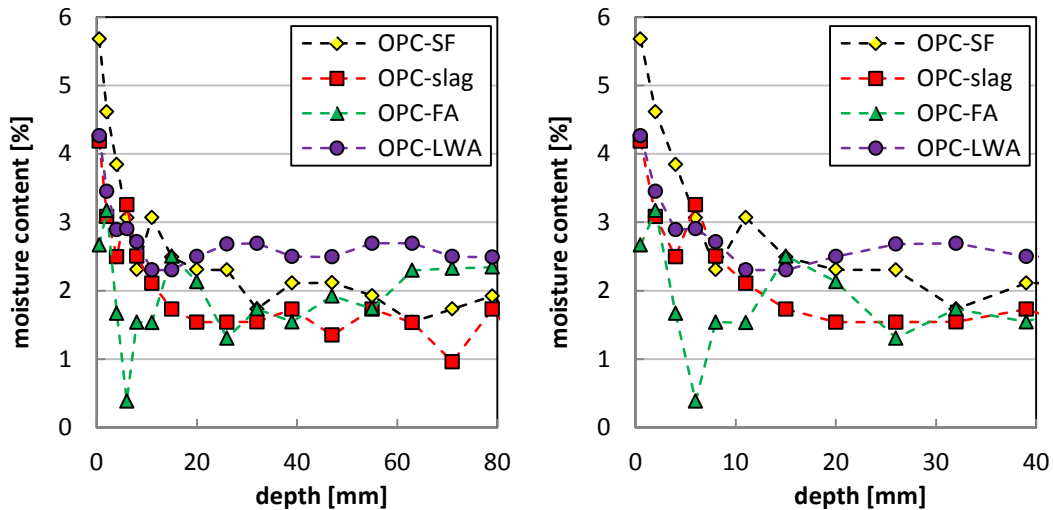


Figure 7: Moisture profiles determined by drying overnight at 105°C of the profile ground powder from the cores drilled from the submerged part of the OPC-SF, OPC-slag, OPC-FA and OPC-LWA concrete beams after 16 years of exposure at the Solsvik exposure site. Left: entire tested profile up to 80 mm from the exposed surface; Right: zoomed into the first 40 mm from the exposed surface.

In Figure 8 the chloride profiles obtained after 16 years of submerged exposure are compared with chloride profiles obtained after 2.5 years of similar exposure supplied by the NPRA [7]. As expected, it can be observed that the chloride ingress has progressed during the time laps 2.5 to 16 years. However, after 2.5 years of exposure the OPC-LWA exhibits the lowest chloride concentrations and OPC-slag the highest, whereas after 16 years the opposite is observed, indicating the concretes have a different aging behavior regarding chloride ingress.

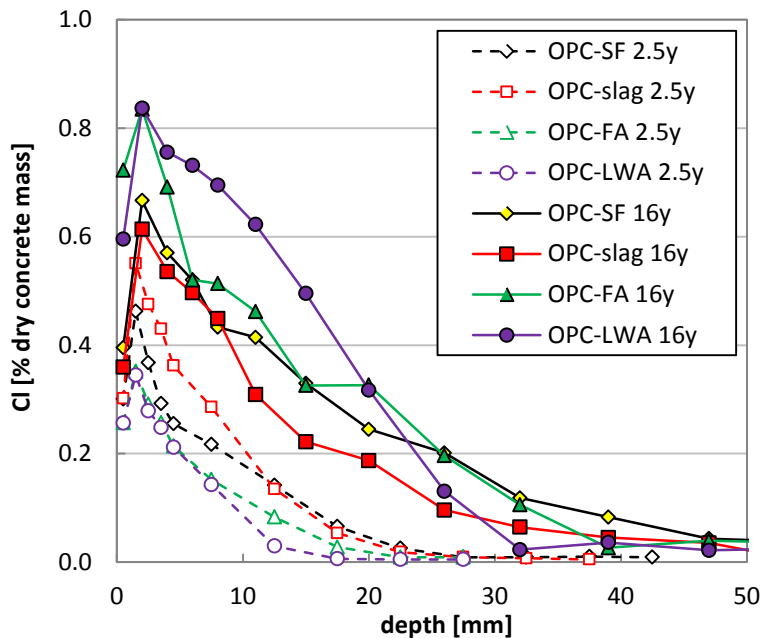


Figure 8: Chloride profiles determined by titration on profile ground cores drilled from the submerged part of the OPC-SF, OPC-slag, OPC-FA and OPC-LWA concrete beams after 2.5 [7] and 16 years of exposure at the Solsvik exposure site.

4.2 ICP-MS

The elemental composition of the profile ground concrete powder was determined by ICP-MS. The aim of this analysis is to relate the elemental changes to changes in the matrix. It is assumed that the aggregates are inert and thereby only the composition of the cement paste changes. However, two facts should be taken into account: (1) ICP-MS analysis is performed on the concrete powder, so also the elements originating from the aggregates and the sand are included, the same aggregates and sand are used for the different concretes which enables comparison, except for OPC-LWA (2) towards the surface the content of fines and cement paste increases due to the wall effect, and this will already on its own lead to variations in the elemental composition.

Figure 9 and Figure 10 depict the variations in Na, Mg, S, Cl and K as a function of depth from the exposed surface determined by ICP-MS. Figure 10 shows the same results as Figure 9, but zooms into the first 20 mm from the exposed surface. Except for the chloride content there are no considerable changes in the measured element concentrations from 10 mm and deeper inwards. Within the first 10 mm from the exposed surface, similar trends are observed for the different concretes tested. Magnesium (Mg) is considerably enriched in the outer most section as its content doubles or triples compared to the background level. A slight increase in sodium (Na) can also be observed in this outer section and remains more or less constant in the rest of the concrete sections. The sulfur (S) content increases in the outer 5 to 10 mm indicating ingress, whereas K decreases gradually towards the surface, indicating leaching.

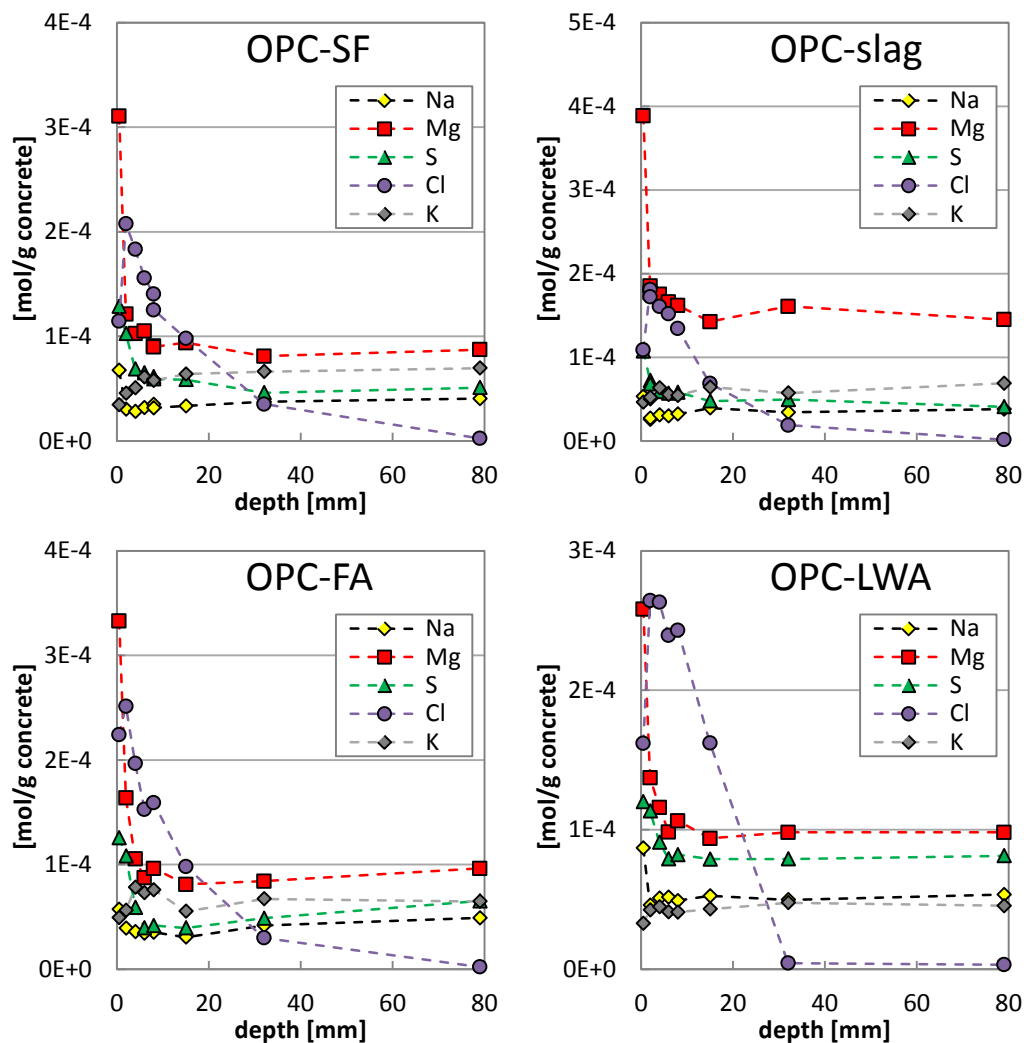


Figure 9: Elemental concentration of Na, Mg, S, Cl and K determined with ICP-MS on the acid solubilized powder from the profile ground OPC-SF, OPC-slag, OPC-FA and OPC-LWA concrete cores.

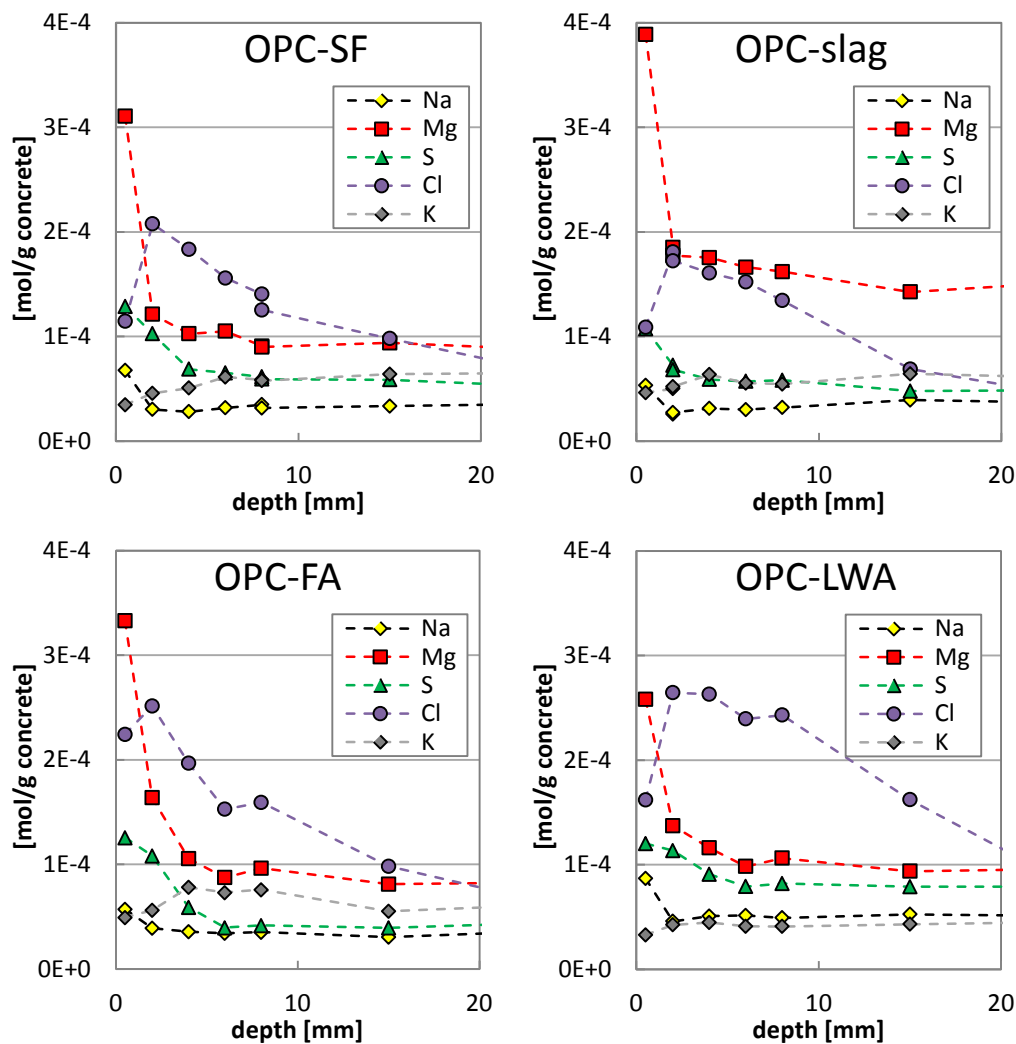


Figure 10: Elemental concentration of Na, Mg, S, Cl and K determined with ICP-MS on the acid solubilized powder from the profile ground OPC-SF, OPC-slag, OPC-FA and OPC-LWA concrete cores; zooming into the first 20 mm from the exposed surface.

Figure 11 shows the concentration of Ca and Cl determined by ICP-MS as well as the therefrom derived Cl/Ca ratio. The Ca content shows an increasing trend towards the surface. This can be partly attributed to the wall effect, leading to increased paste content towards the surface. This effect is prominent for Ca as it is one of the main components of cement paste. It should be noted that the background Ca value for OPC-LWA is higher compared to the other concretes which might be attributed to the higher matrix content in this particular concrete.

Assuming that Ca relates to the cement content in the concrete, the Cl/Ca ratio would reflect variation of the Cl in the paste. However, it should be kept in mind that precipitation or leaching of Ca rich phases, e.g. calcium carbonate and calcium hydroxide, might complicate the interpretation of these profiles relative to the Ca content.

The Cl/Ca profiles of the different tested concretes, show a lower Cl/Ca ratio near the surface (0-1 mm section), followed by a zone of in which the highest chloride concentrations are reached (1-10 mm) instead of a single peak as observed in the chloride profiles. After the maximum zone the chloride content decreases when moving further inwards from the exposed surface.

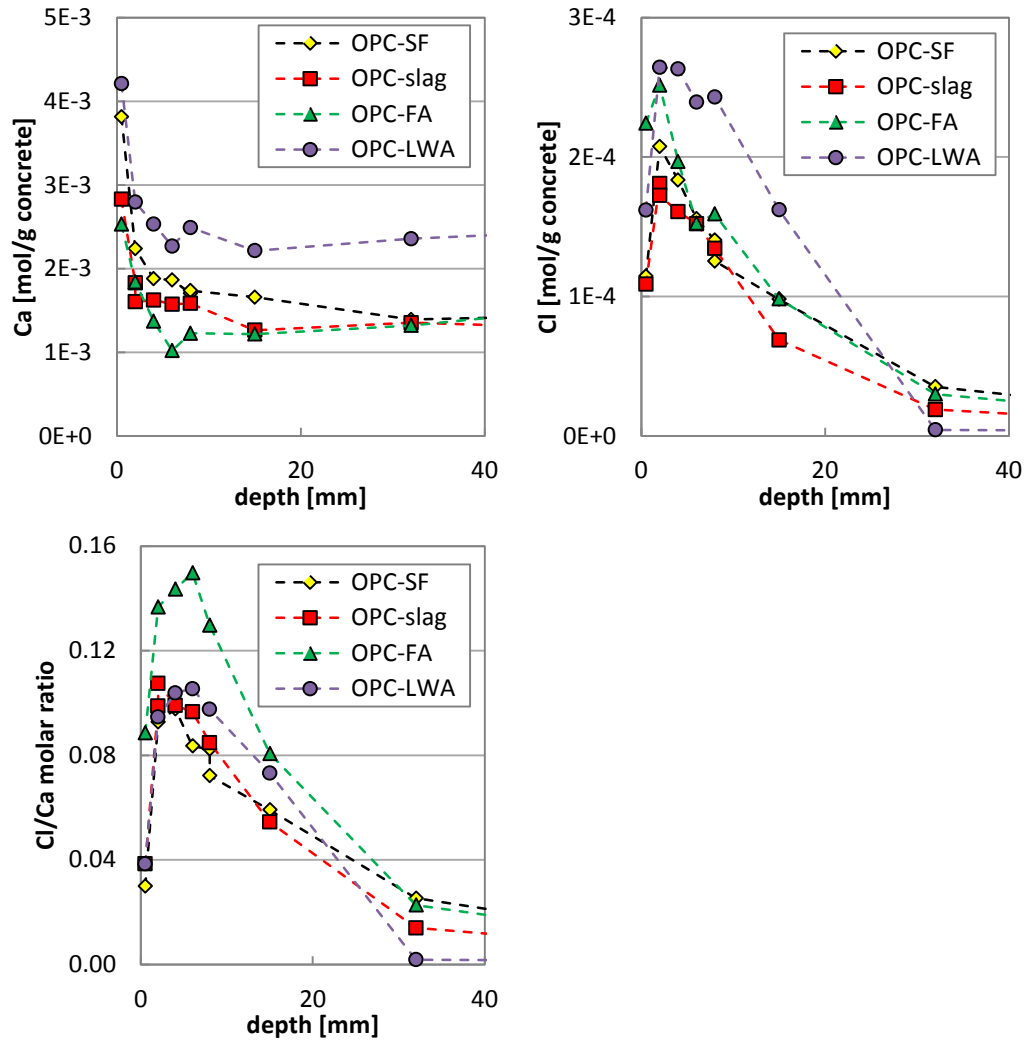


Figure 11: Concentration of Ca, Cl and Cl/Ca ratio determined with ICP-MS on the acid solubilized powder from the profile ground OPC-SF, OPC-slag, OPC-FA and OPC-LWA concrete cores.

In Figure 12 the chloride profiles determined by titration are compared with the chloride profiles determined by ICP-MS. It should be noted that the same acid solubilized profile ground powder is used for both analyses. The results are relatively similar for both methods except for the OPC-LWA sample. The reason for this is unknown. For the other tested concretes ICP-MS tends to slightly overestimate the chloride content compared to titration.

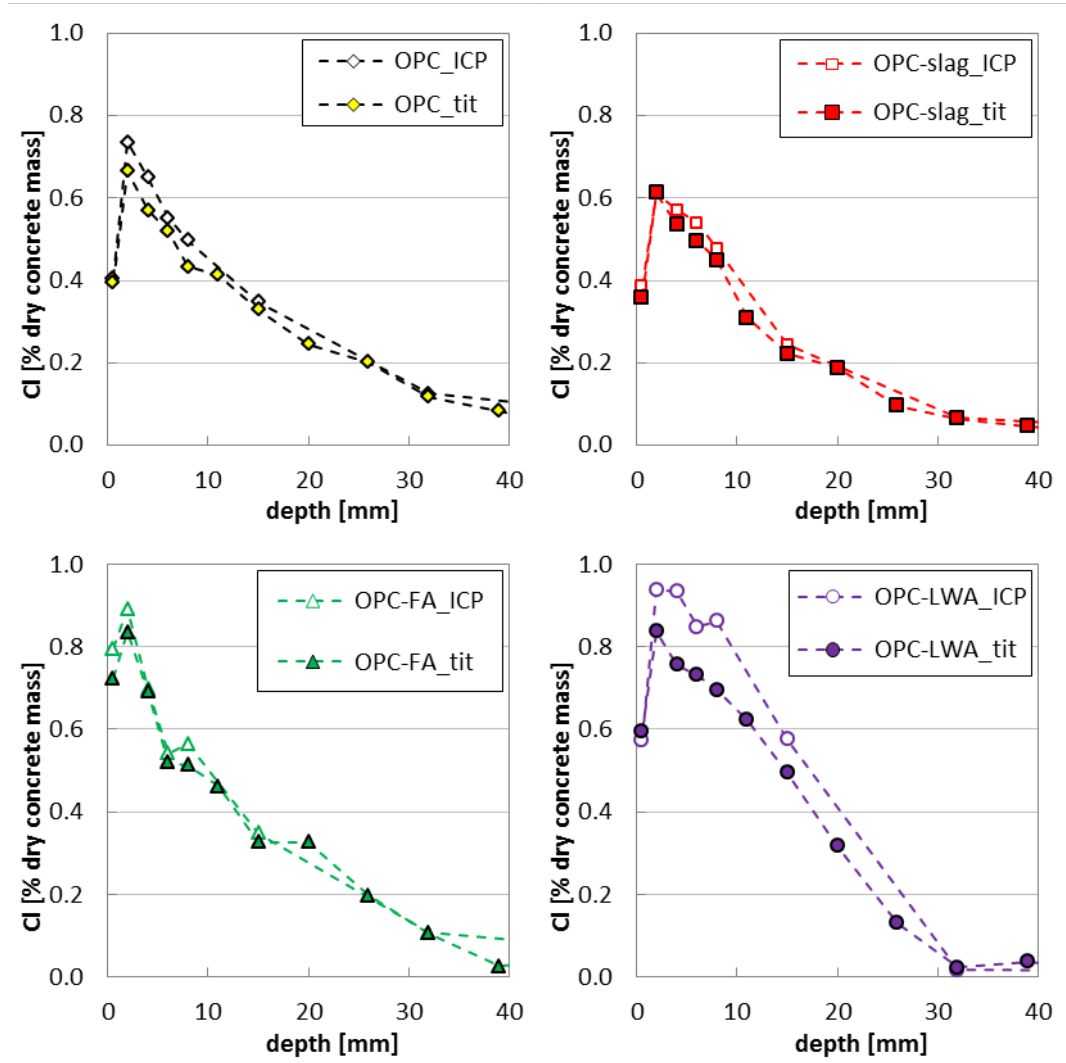


Figure 12: Comparison of the chloride profiles determined by titration and ICP-MS on profile ground cores drilled from the submerged part of the OPC-SF, OPC-slag, OPC-FA and OPC-LWA cores.

4.3 TGA

Figure 13 to Figure 16 show a selection of TG (thermogravimetric) and DTG (differential thermogravimetric) curves for profile ground sections of the examined concrete cores. Based on these curves weight losses in different temperature intervals were determined.

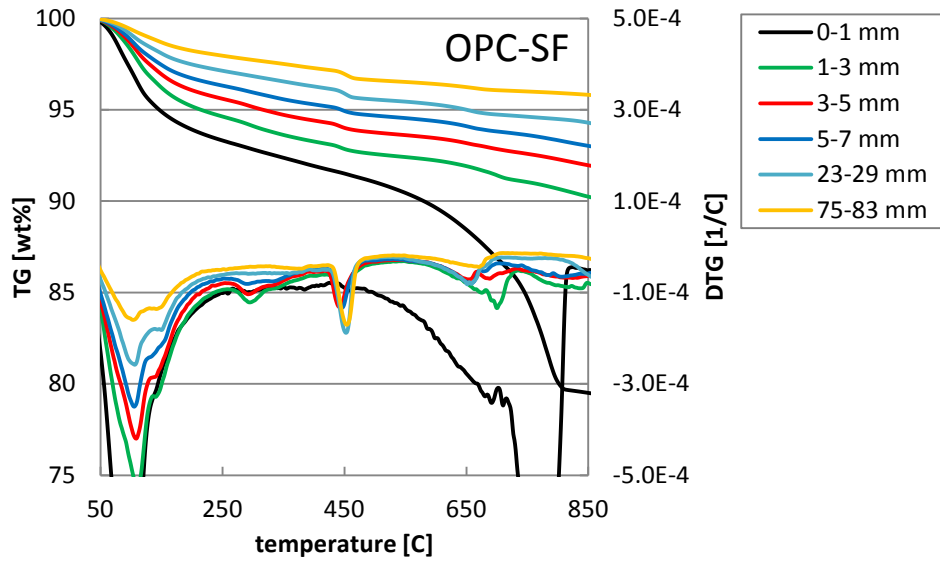


Figure 13: The TG and the DTG curves determined by TGA for different sections of the profile ground OPC-SF concrete core.

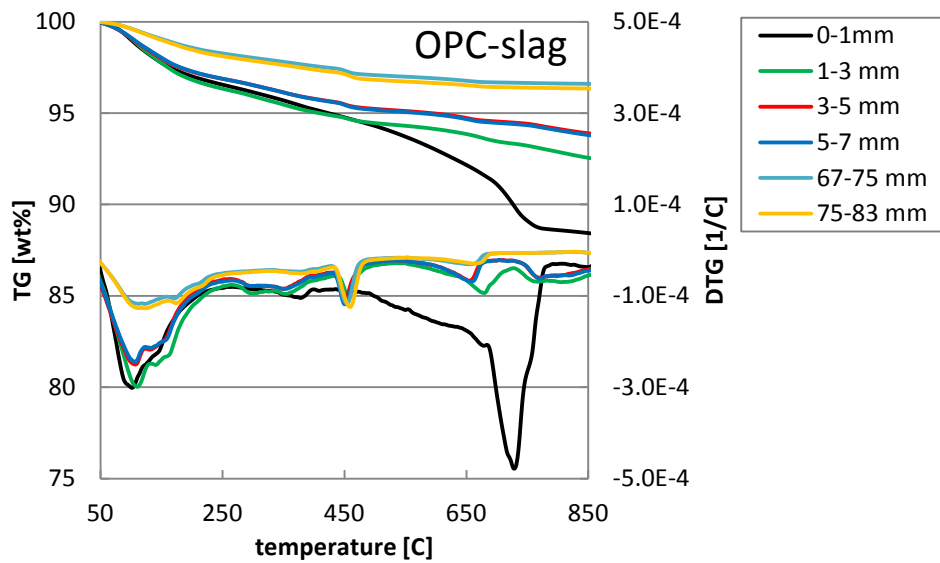


Figure 14: The TG and the DTG curves determined by TGA for different sections of the profile ground OPC-slag concrete core.

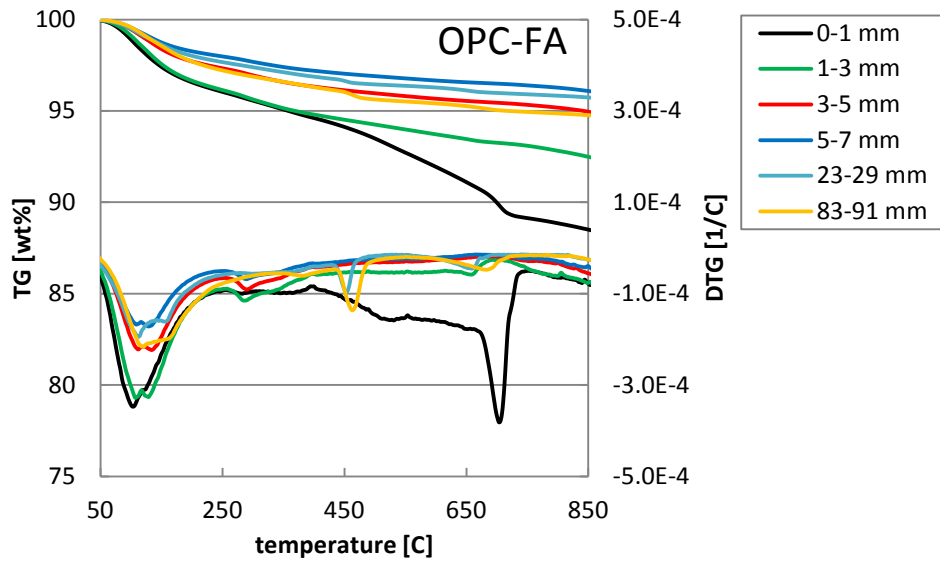


Figure 15: The TG and the DTG curves determined by TGA for different sections of the profile ground OPC-FA concrete core.

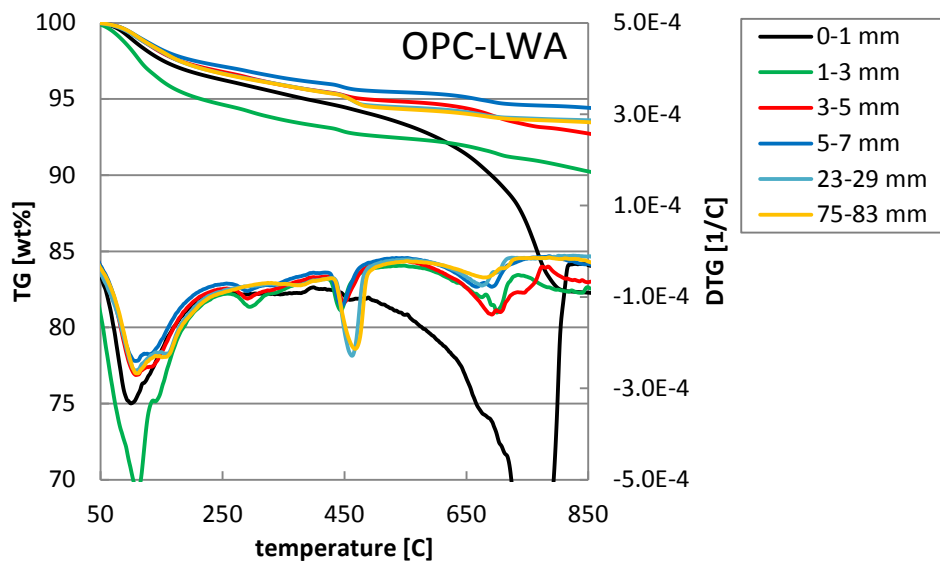


Figure 16: The TG and the DTG curves determined by TGA for different sections of the profile ground OPC-LWA concrete core.

The Portlandite content is related to the mass loss in the 400-500°C temperature interval as described in the experimental chapter. The variation of Portlandite as function of the depth from the exposed surface is depicted in Figure 17. For all tested concretes the Portlandite content decreases towards the exposure surface, even though the paste content increases in that zone due to the wall effect. This indicates severe leaching of Portlandite.

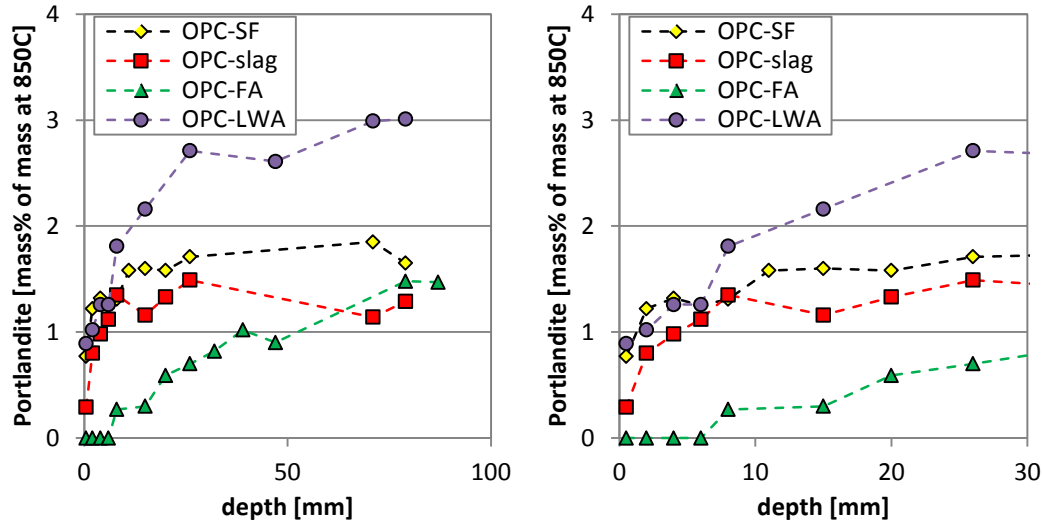


Figure 17: The amount of Portlandite determined by TGA for different sections of the profile ground OPC-SF, OPC-FA, OPC-slag and OPC-LWA cores. Left: entire tested profile up to 80 mm from the exposed surface ; Right: zoomed into the first 30 mm from the exposed surface.

The Portlandite profiles for OPC-SF and OPC-slag are relatively similar; showing a leaching profile in the first 10 mm from the exposure surface and a relative constant Portlandite content deeper inwards. OPC-LWA and OPC-FA exhibit a lowering of the Portlandite content in respectively the first 30 and 50 mm from the exposure surface. This might indicate more severe leaching, however in the case of OPC-FA the continued pozzolanic reaction of the fly ash might also contribute to lowering of the Portlandite content.

The water loss measured in the temperature interval 40-450°C by TGA as function of the depth from the exposed surface for the different tested concretes is shown in Figure 18. All concretes exhibit an increase in the water content towards the exposure surface. This might be due to both a higher amount of bound water due to the higher cement paste content (wall effect) at the surface and better accessibility of moisture in the vicinity of the exposed surface.

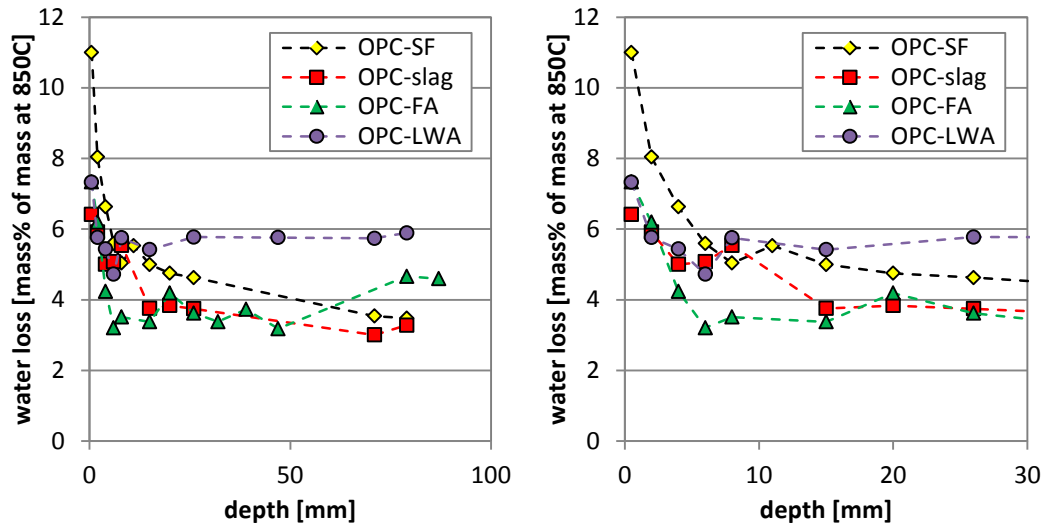


Figure 18: The amount of water loss determined by TGA for different sections of the profile ground OPC-SF, OPC-FA, OPC-slag and OPC-LWA cores. Left: entire tested profile up to 80 mm from the exposed surface; Right: zoomed into the first 30 mm from the exposed surface.

The carbonate content based on the weight loss measured in the temperature interval 550-800°C is shown as function of the depth from the exposed surface for the different tested concretes in Figure 19. For all concretes only the outer section (0-1 mm) seems to have a considerable increase in the carbonate content. This can also be seen from Figure 13 in the case of OPC-SF concrete.

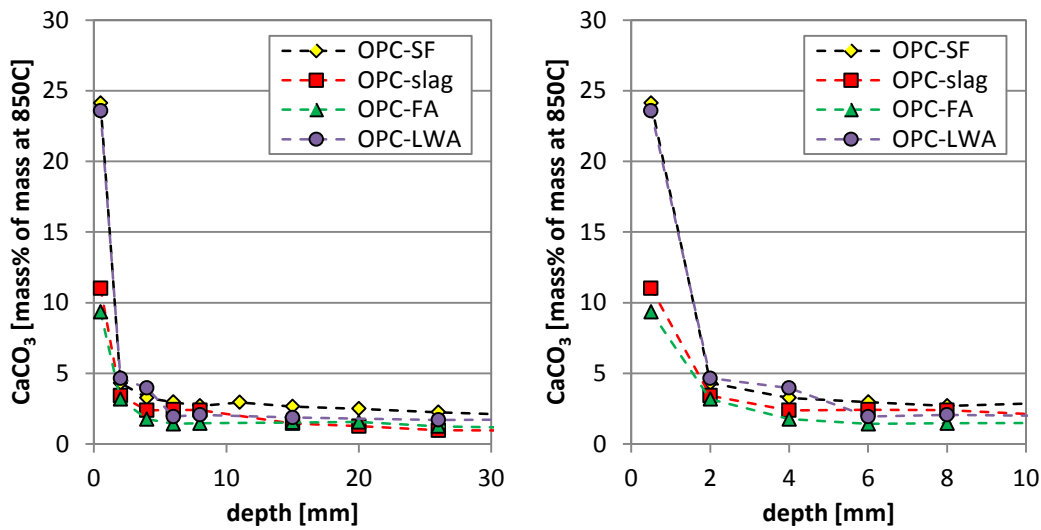


Figure 19: The amount of CaCO₃ determined by TGA for different sections of the profile ground OPC-SF, OPC-FA, OPC-slag and OPC-LWA cores; zoomed into the first 30 mm from the exposed surface.

4.4 SEM-EDS

The elemental composition of an area of $125 \times 165 \mu\text{m}$ was determined by SEM-EDS. With the aim to relate the elemental changes to the paste content, elemental changes are expressed relative to the Ca content. Figure 20 shows the Cl/Ca profiles as function of the depth from the exposed surface. Similar observations can be made for the different tested concretes. The Cl/Ca ratio near the surface is very low and it increases after 200-300 μm to reach a maximum at 1-4 mm from the surface. A zone of maximum Cl/Ca ratio is observed rather than a peak, which is in-line with the ICP-MS observations.

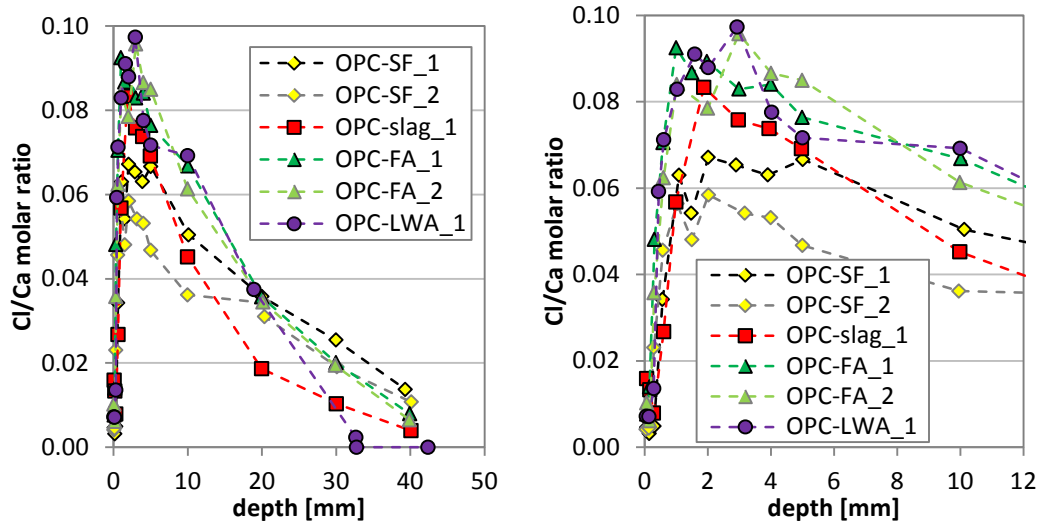


Figure 20: Cl/Ca ratio profiles determined with SEM-EDS on polished thin sections by analyzing an area ($125 \times 165 \mu\text{m}$) at different depths from the exposed surface for the OPC-SF, OPC-FA, OPC-slag and OPC-LWA cores.

Figure 21 presents the S/Ca ratio as function of the depth from the exposed surface. Again the different tested concretes seem to behave similarly. The sulfur content near the surface is very low, the sulfur concentration increases from 200-300 μm from the surface to reach a maximum at between 0.5 and 0.8 mm from the surface, and decreases back to the background level from approx. 2 mm from the surface. For the S/Ca ratio a clear peak behavior is observed in contradiction of the Cl/Ca ratio.

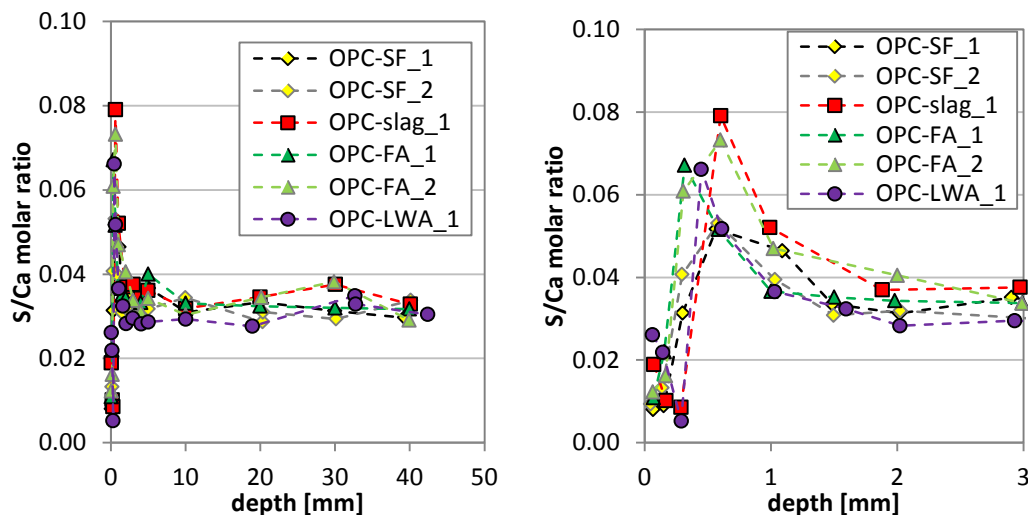


Figure 21: S/Ca ratio profiles determined with SEM-EDS on polished thin sections by analyzing an area ($125 \times 165 \mu\text{m}$) at different depths from the exposed surface for the OPC-SF, OPC-FA, OPC-slag and OPC-LWA cores.

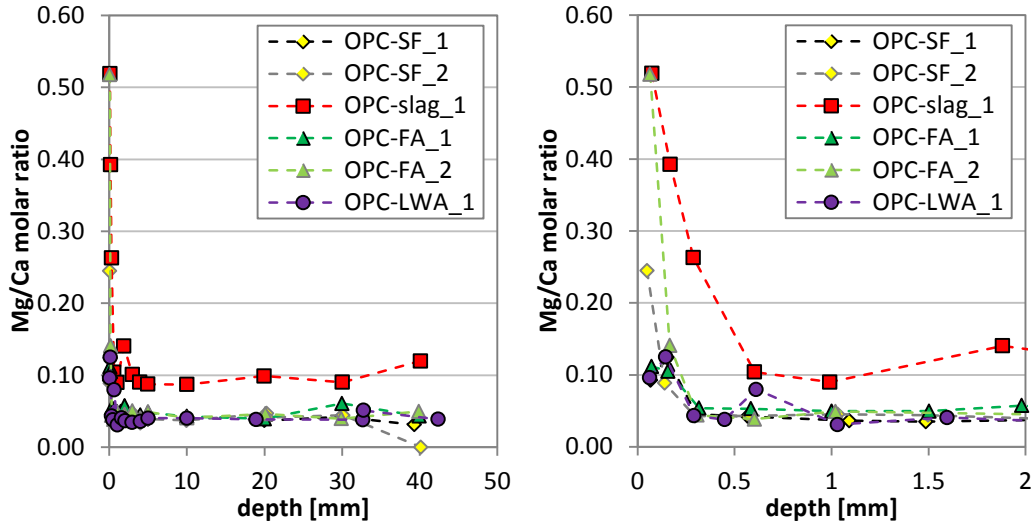


Figure 22: Mg/Ca ratio profiles determined with SEM-EDS on polished thin sections by analyzing an area (125x165 μm) at different depths from the exposed surface for the OPC-SF, OPC-FA, OPC-slag and OPC-LWA cores.

Figure 22 shows the Mg/Ca ratio as function of the depth from the exposed surface. The zone within 0.5 mm from the surface which has low Cl/Ca and S/Ca values seems to be enriched in Mg. The background Mg/Ca level is higher for the OPC-slag concrete. This is most likely caused by the Mg content in the slag.

Figure 23, Figure 24, Figure 25 and Figure 26 show Cl/Ca, S/Ca and Mg/Ca molar profiles determined by SEM-EDS for the different tested concretes. From these figures one can see that the Mg/Ca peak at the surface precedes the S/Ca peak which in turn tends to precede the Cl/Ca maximum. There is a slight overlap between the S/Ca and Cl/Ca peak, but the S/Ca ratio tends to decrease prior to the Cl/Ca ratio reaching the maximum zone. In addition, the zone of high Mg/Ca and low Cl/Ca and S/Ca ratio seems to coincide, indicating that this zone is chemically greatly altered.

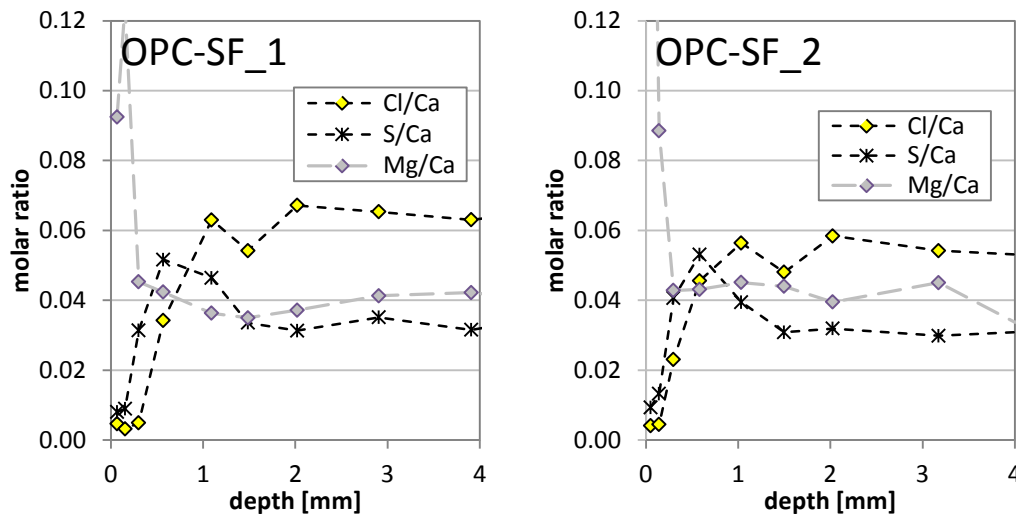


Figure 23: Cl/Ca, S/Ca and Mg/Ca molar ratio profiles determined with SEM-EDS on polished thin sections by analyzing an area (125x165 μm) at different depths from the exposed surface for the OPC-SF core. Two parallel tracks were analysed OPC-SF_1 and OPC-SF_2.

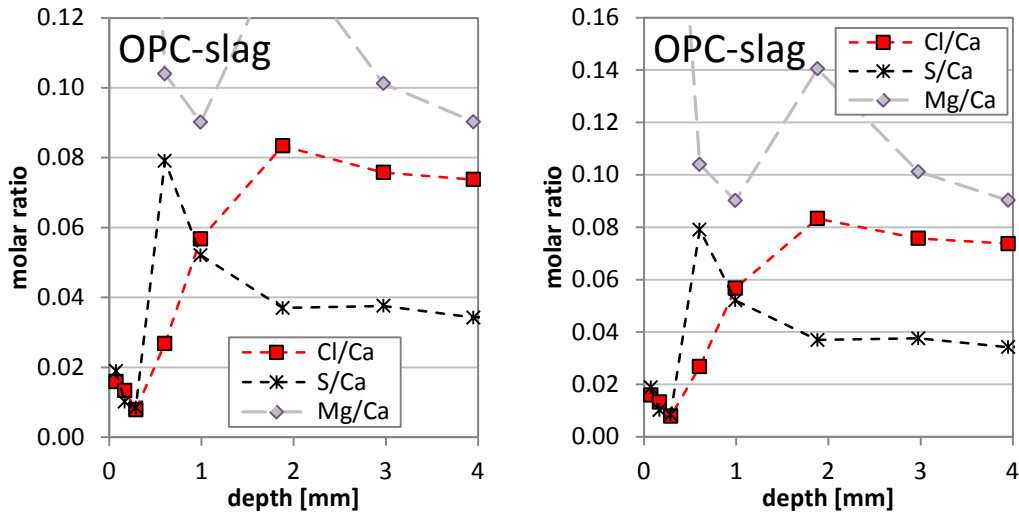


Figure 24: Cl/Ca, S/Ca and Mg/Ca molar ratio profiles determined with SEM-EDS on polished thin sections by analyzing an area (125x165 μm) at different depths from the exposed surface for the OPC-slag core. One track was analyzed, but an additional graph with larger range on the y-axis is added due to include the Mg (most likely present in the slag).

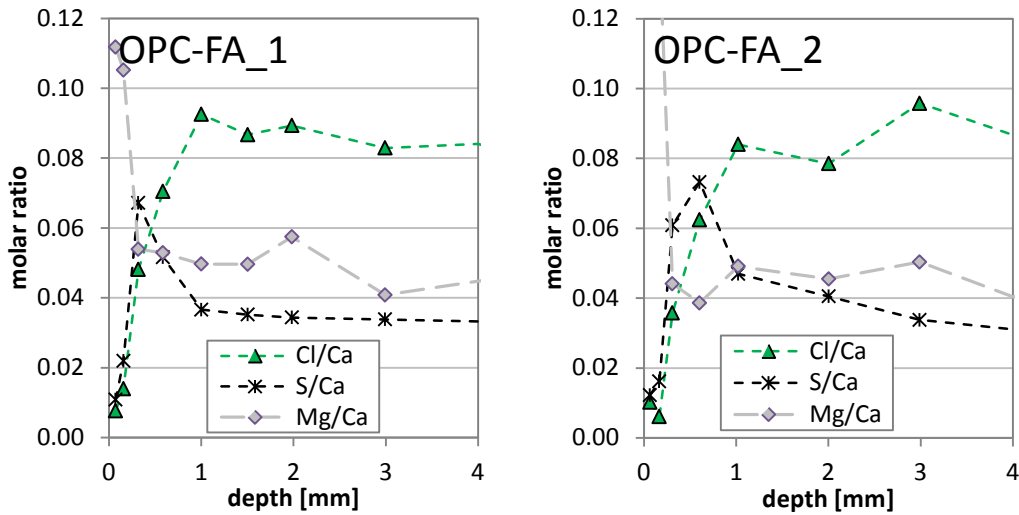


Figure 25: Cl/Ca, S/Ca and Mg/Ca molar ratio profiles determined with SEM-EDS on polished thin sections by analyzing an area (125x165 μm) at different depths from the exposed surface for the OPC-FA core. Two parallel tracks were analysed OPC-FA_1 and OPC-FA_2.

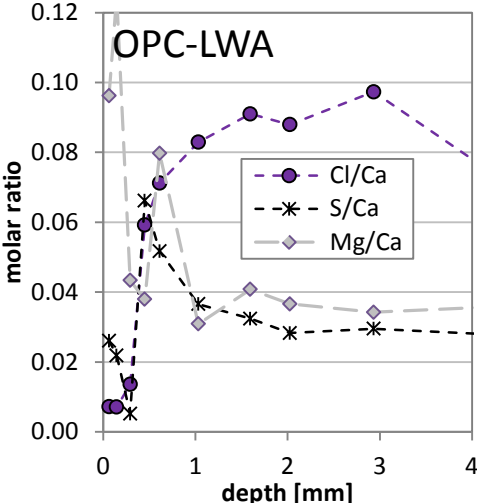


Figure 26: Cl/Ca, S/Ca and Mg/Ca molar ratio profiles determined with SEM-EDS on polished thin sections by analyzing an area (125x165 μm) at different depths from the exposed surface for the OPC-LWA core.

The Cl/Ca and S/Ca profiles obtained with SEM-EDS and ICP-MS are compared in Figure 27 and Figure 28, respectively. It should be noted that SEM-EDS profiles are defined based on the analysis a path way with a width of 165 μm from the surface deeper into the polished thin section. Hence the representativeness of this data can be discussed. However, the SEM-EDS technique allows studying the relation between the variations of the different elements on a detailed spatial scale. ICP-MS on the other hand has a limited spatial scale (1-2 mm), but is more representative for the concrete core as the analysis is performed on a homogenized profile ground sample.

From Figure 27 it can be seen that SEM-EDS seems to underestimate the Cl/Ca ratio at higher Cl/Ca values compared to ICP-MS. However, similar curve shapes are obtained by both methods. The underestimation of the SEM-EDS results might be partly caused by the samples preparation of the polished thin section: where the drying prior to epoxy impregnation will lead to precipitation of ions from the pore solution, while during the polishing steps ions might be washed out.

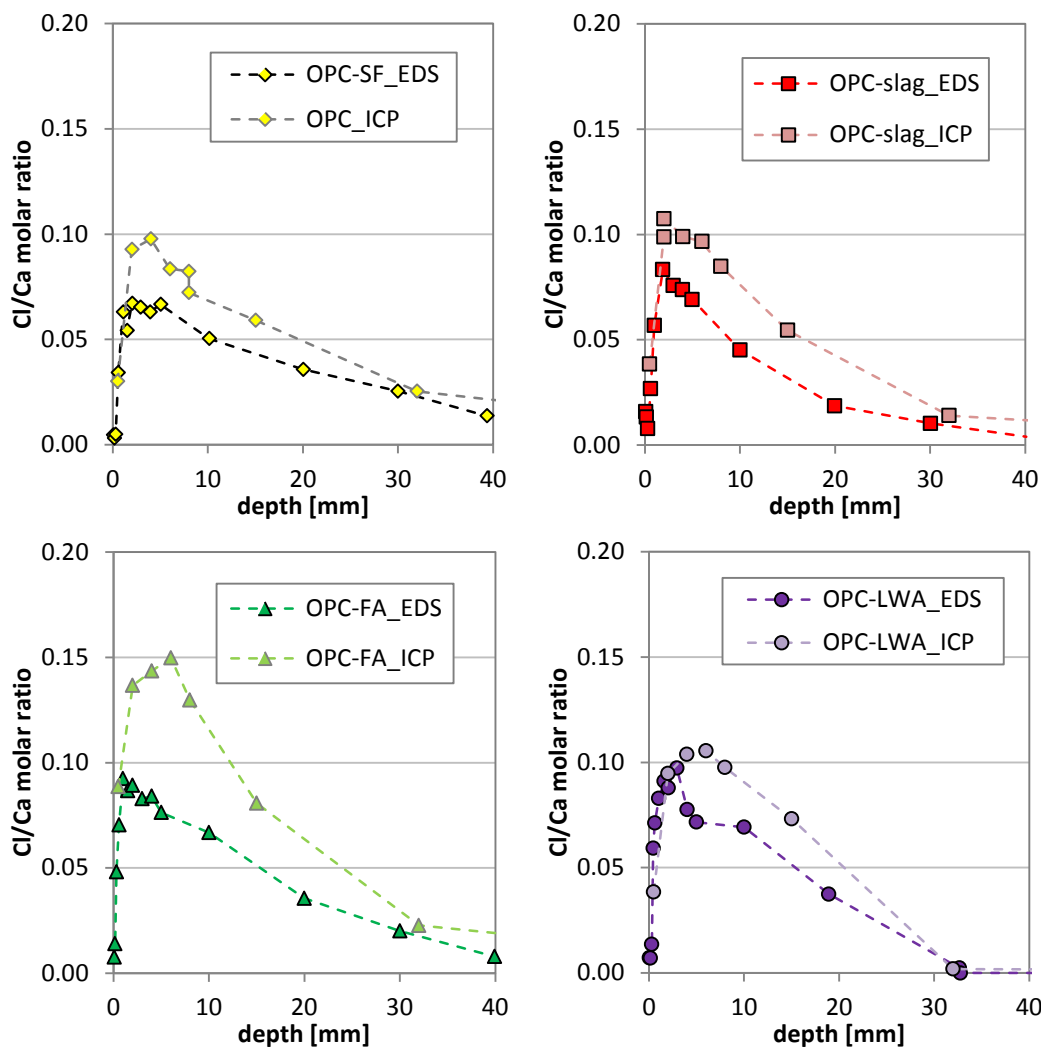


Figure 27: Comparison of the Cl/Ca ratio profiles determined by ICP-MS on profile ground cores with the profiles determined by SEM-EDS on polished thin sections for the OPC-SF, OPC-slag, OPC-FA and OPC-LWA cores.

From Figure 28 it can be seen that SEM-EDS and ICP-MS measure similar background levels of the S/Ca ratio. SEM-EDS seems to be more appropriate to catch the peak behavior of the S/Ca profile near the surface which is overseen by ICP-MS. ICP-MS seems to show a deeper ingress of the S compared to SEM-EDS. This might be either due to the choice of a less representative path for the SEM-EDS measurements or due to possible inaccuracy in the profile grinding process as the sulfur peak occurs at 1 mm which is the grinding limit between the first two sections (0-1 mm and 1-3 mm).

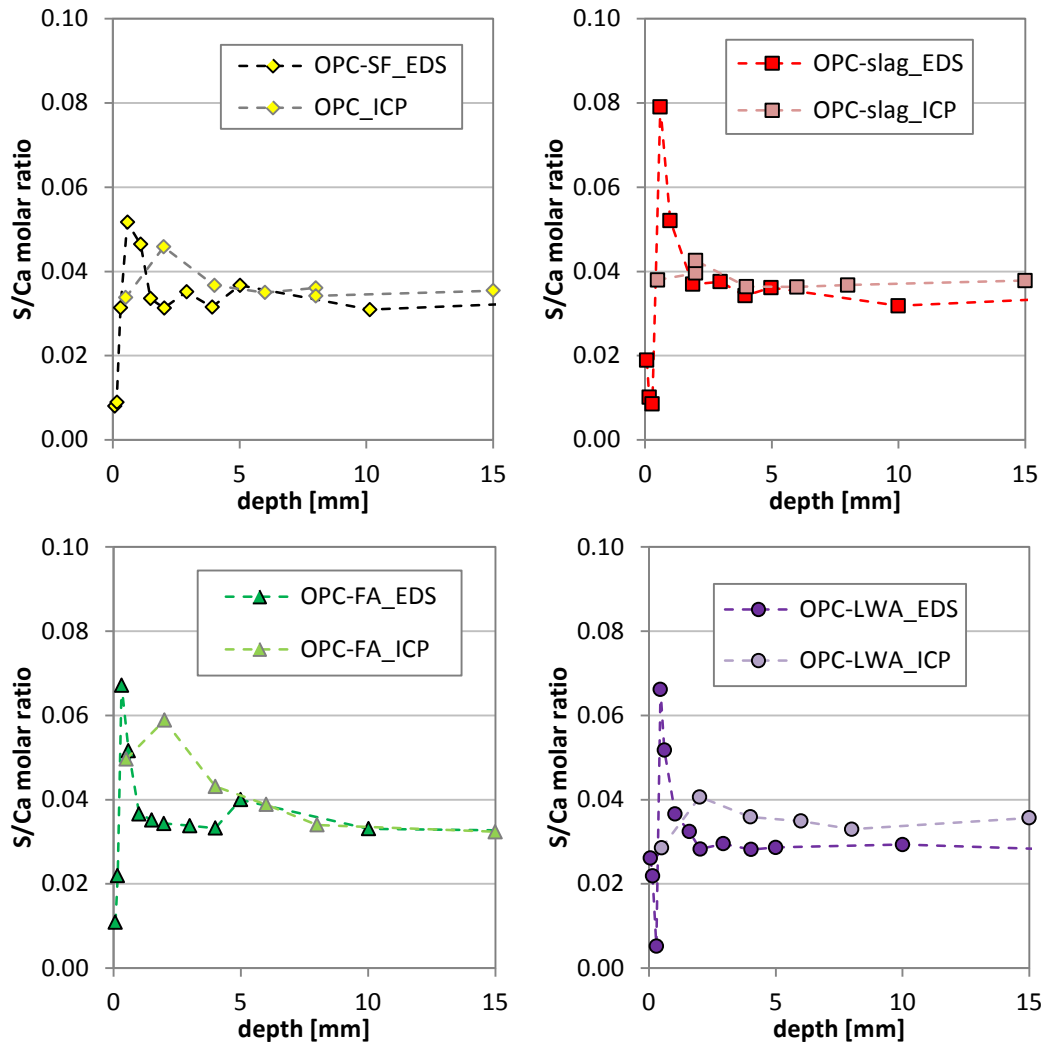


Figure 28: Comparison of the S/Ca ratio profiles determined by ICP-MS on profile ground cores with the profiles determined by SEM-EDS on polished thin sections from the OPC-SF, OPC-slag, OPC-FA and OPC-LWA cores.

Figure 29 shows the elemental maps approx. 3x11 mm for the OPC-LWA concrete taken from the exposed surface and inwards. The intensity of the color in the SEM-EDS maps is related to the relative concentration of the element. From this figure one can observe the following:

- Ca represents the matrix and a Ca-rich deposit can be observed on the surface.
- S and Cl are enriched in the cement paste (coinciding with the Ca map), however S and Cl concentrations are low just at the surface. The S and Cl content seem to increase at approx. 100 μm from the surface, but the S content decreases within 1 mm back to the background level whereas the Cl content remains high deeper inwards from the surface, throughout the whole map.
- Mg seems to present at the surface (not so clear) and in some of the minerals of the aggregates.
- Aggregates present in the map consist mainly of Si, Al, Na and K. In addition some Mg and Fe containing minerals are observed. This should be kept in mind when studying profiles of these elements relative to Ca.
- LWA (particle in the bottom left) does not seem to enrich in Cl, as the LWA particle has a similar intensity in the Cl map compared to the conventional aggregates.

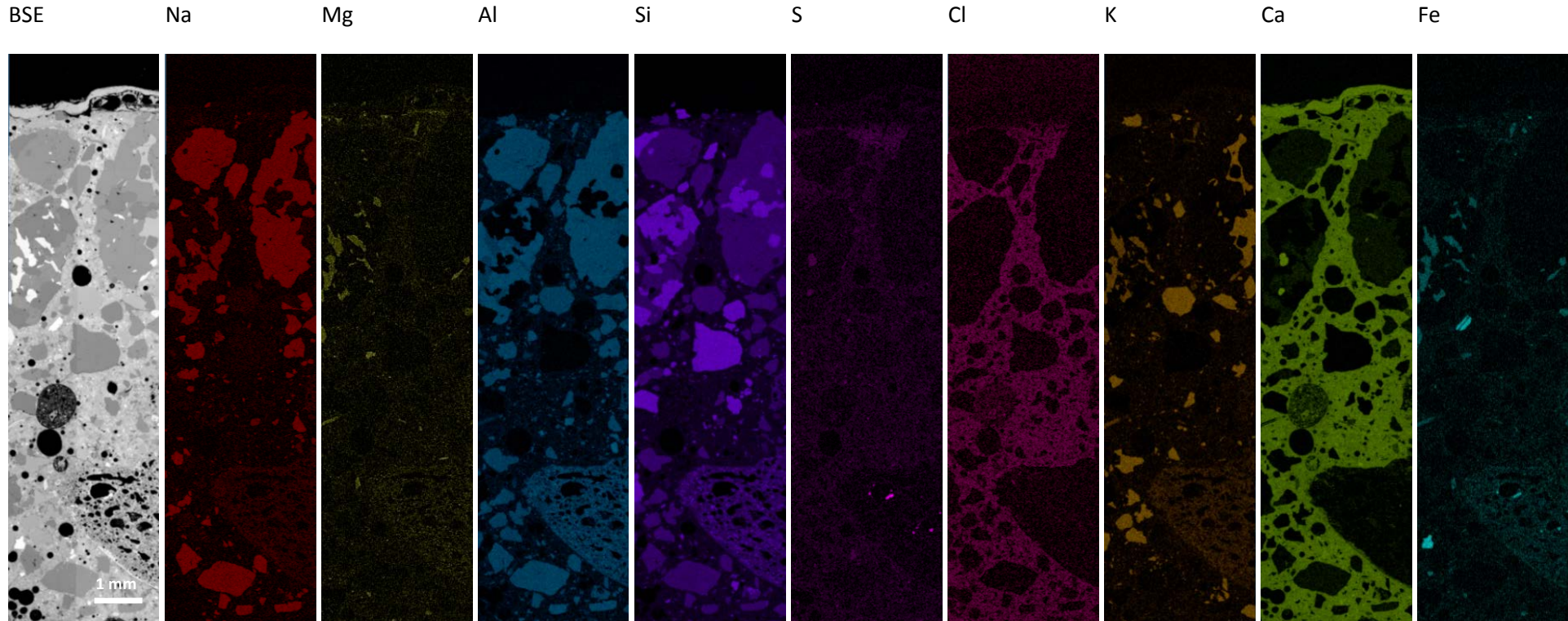


Figure 29: Elemental maps of approx. 3x11 mm taken from the exposed surface and inwards for the OPC-LWA concrete.

4.5 Microscopy

Microscopy allows the study of the spatial distribution of carbonation near the surface on thin sections. Figure 30 shows the discoloration of the paste which is a consequence of carbonation of the cement paste for OPC-SF, OPC-slag and OPC-FA. OPC-LWA was not included in this part of the study. Table 4 gives an overview over the estimated carbonation depth of the paste in the tested thin sections.

In addition to the paste carbonation, a white layered deposit can be observed on the concrete surface in Figure 30 which is build up out of calcium carbonate and brucite deposits. It should be noted that the submerged part of the concrete beams at Solsvik were covered with shells and other sea life when they were taken up on the dock.

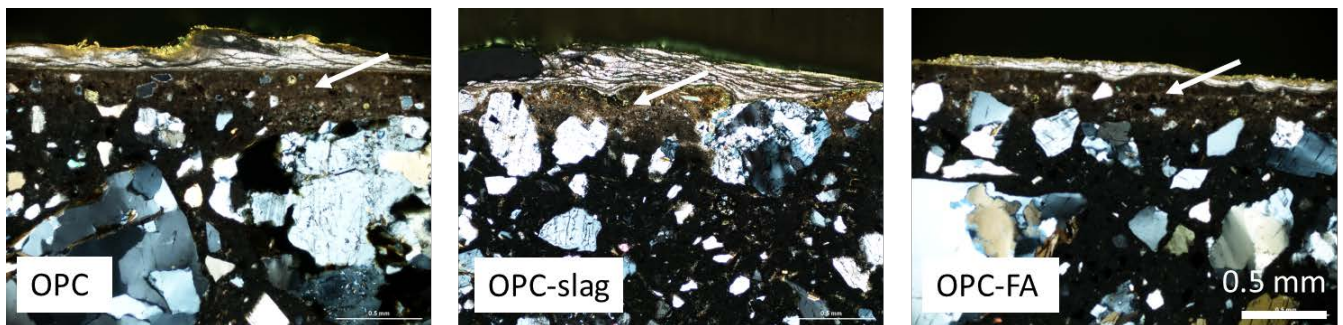


Figure 30: Micrographs taken with polarized light of the exposed surface on fluorescent epoxy impregnated polished thin sections from the OPC-SF, OPC-slag, and OPC-FA cores. The discoloration of the cement paste at the surface (white arrow) indicates carbonation.

Table 4: Estimated carbonation depth based on the investigation of the polished thin sections from the OPC-SF, OPC-slag, and OPC-FA cores.

Sample	Carbonation depth
OPC-SF	0.4-0.8 mm
OPC-slag	0.2-0.4 mm
OPC-FA	0.1-0.2 mm

Figure 31 shows image taken with ultraviolet light of the fluorescence impregnated thin sections near the exposed surface. The darker tone of the concrete near the surface indicates a densification of the cement paste. This suggests that the concrete surfaces did not become more porous after being submerged for 16 years in sea water.

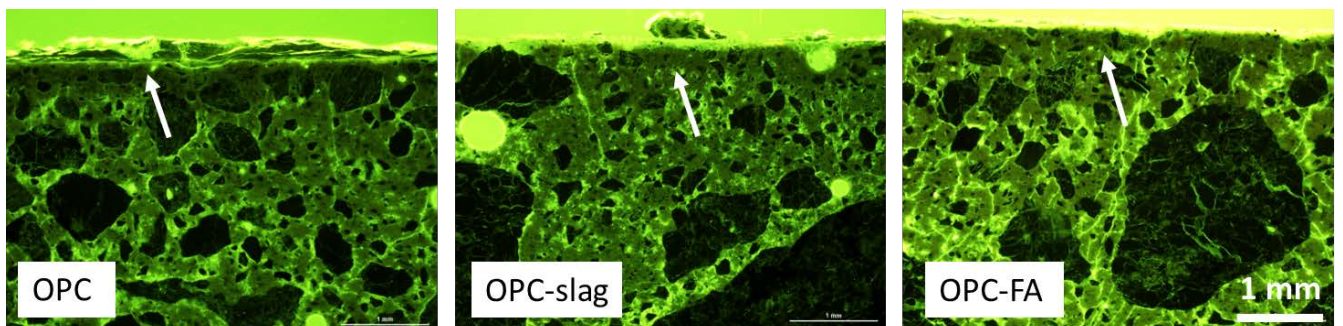


Figure 31: Micrographs taken with ultraviolet light of the exposed surface on fluorescent epoxy impregnated polished thin sections from the OPC-SF, OPC-slag, and OPC-FA cores. The darker tone of the cement paste near the surface (white arrow) indicates a densification.

4.6 PF-method

Figure 32 shows the suction porosity profiles determined for drying at 50°C and 105°C. The suction porosity is larger for drying at 105°C than for drying at 50°C, as expected. More adsorbed as well as bound water is removed when drying at 105°C compared to 50°C. The trends of the suction porosity profiles at both temperatures are however similar. For all tested concretes except for the OPC-SF, there is a slight trend of increase in suction porosity towards the exposed surface, which might be due to the higher paste content (wall effect) towards the exposed surface. The higher suction porosity of the OPC-LWA compared to the other tested concretes, might also be attributed to the higher paste content in this particular concrete.

When comparing the concretes with the different binders in the range of 40-80 mm and for the split sample (indicated at 100 mm), the following order of decreasing suction porosity is observed: OPC-FA, OPC-SF, and OPC-slag.

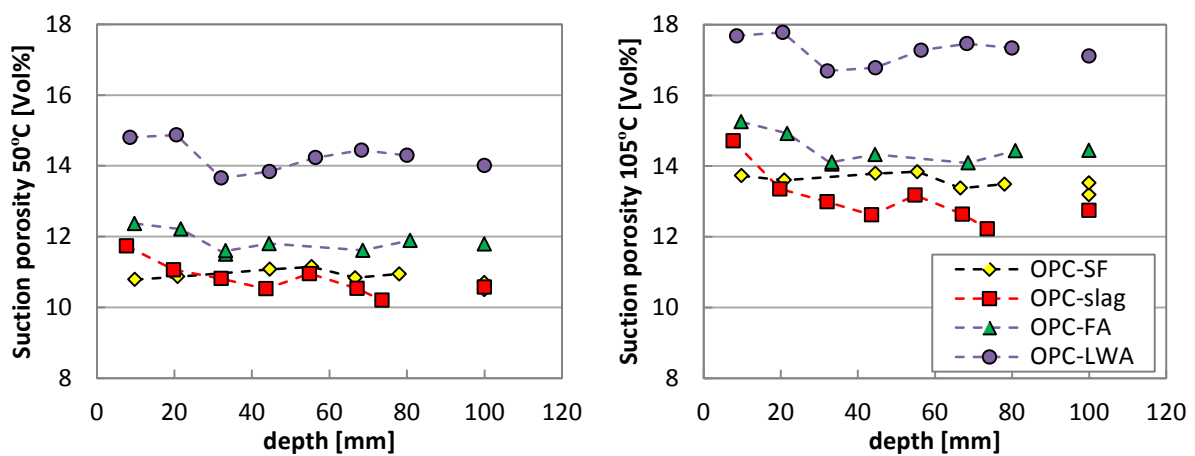


Figure 32: The suction porosity for drying at 50°C (Left) and 105°C (Right) of the sawn samples taken at different depths from the surface as well as a split bulk sample (indicated at 100 mm depth) for the OPC-SF, OPC-slag, OPC-FA and OPC-LWA concrete cores.

The degree of capillary saturation (DCS) profiles are shown in Figure 33. For all tested concretes, there is a slight trend of decreasing DCS when moving deeper into the concrete. This indicates self-desiccation of the concrete, meaning that hydration of the binders has reduced the amount of free water and that this could not be compensated for by external water. From 30 mm from the surface and inwards the DCS remains more or less constant.

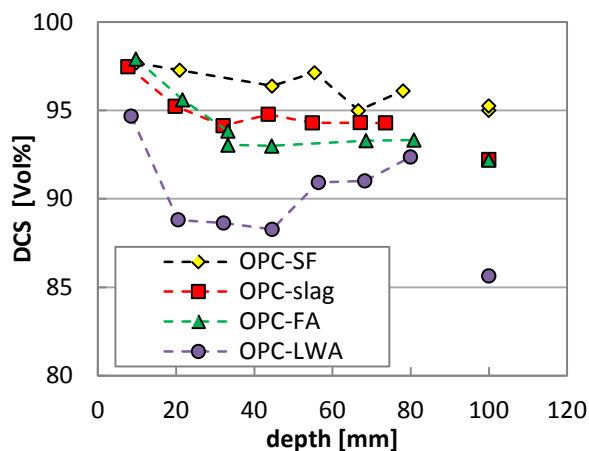


Figure 33: Degree of capillary saturation (DCS) for the sawn samples taken at different depths from the surface as well as a split bulk sample (indicated at 100 mm depth) for the OPC-SF, OPC-slag, OPC-FA and OPC-LWA concrete cores.

The DCS of the split samples (shown at 100 mm depth) is slight lower than the DCS at 40-80 mm for OPC-SF, OPC-slag and OPC-FA. This indicates that during the cutting of the samples with a water lubricated saw, additional water was introduced to the samples.

The DCS profile of the OPC-LWA concrete is peculiar. Further research is needed to better understand the behavior of the OPC-LWA during PF testing. It should be noted that the discs used for these measurements were only 10 mm thick. This is considerably thinner than the normally recommended 40 mm [4]. The reducing the thickness of the discs will result in an increase in the amount of cut light weight aggregate particles (LWA) which are exposed. The filling of pores in the LWA during sawing and capillary suction measurements might influence the results.

Figure 34 shows the macro porosity profiles for the different tested concretes. It should be noted that the samples have too small dimensions to perform proper macro pore measurements. The concretes with the different binders, OPC-SF, OPC-slag and OPC-FA, seems to have a quite constant volume of macro pores both in the sawn and split samples. OPC-LWA has a considerably higher volume of macro pores, which indicates that the macro porosity of the light weight aggregates is filled during the pressurizing of the samples. This could possibly be avoided by using larger samples. The LWA aggregates have a dense sintered shell, which if not cut might prevent the ingress of water. However to conclude on this further research is needed.

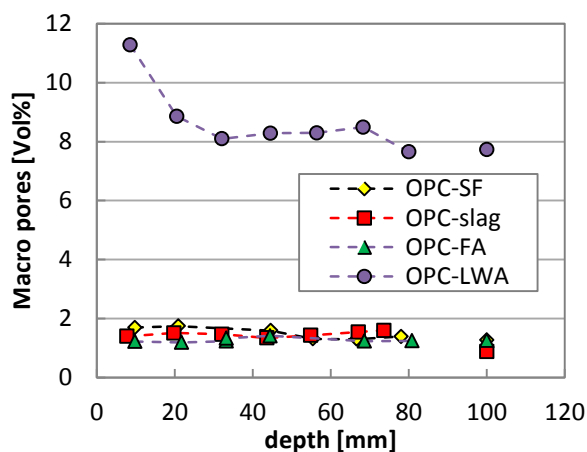


Figure 34: Macro porosity for the sawn samples taken at different depths from the surface as well as a split bulk sample (indicated at 100 mm depth) for the OPC-SF, OPC-slag, OPC-FA and OPC-LWA concrete cores.

4.7 RH

The relative humidity (RH) profiles for the different tested concretes are shown in Figure 35. No clear trend can be observed from these profiles. The split samples (indicated at 100 mm depth) show a lower RH compared to the profiles which might indicate that the cutting with a water cooled saw interfered considerably with the results. These split samples do however indicate self-desiccation of the concrete. It should be noted that the relative humidity in a saturated concrete samples is not 100% due to the high ionic strength of the pore solution. However values below 95% RH do give an indication of self-desiccation.

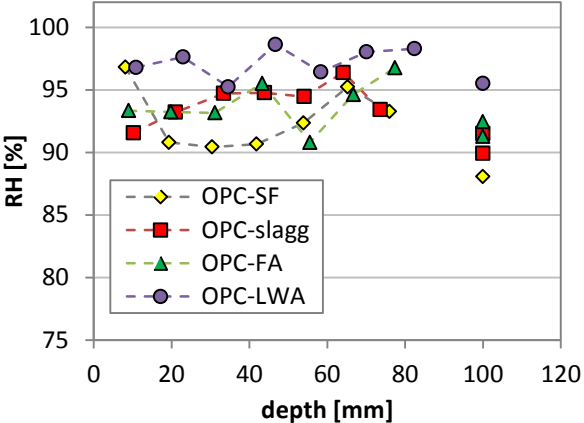


Figure 35: Relative humidity (RH) for the crushed sawn samples taken at different depths from the surface as well as a split bulk sample (indicated at 100 mm depth) for the OPC-SF, OPC-slag, OPC-FA and OPC-LWA concrete cores

5 Discussion

Chloride profiles

- Techniques:

Chloride profiles were determined by titration, ICP-MS and SEM-EDS. The titration and ICP-MS were both performed on acid solubilized profile ground concrete powder. Both techniques gave similar results, even though ICP-MS tended to slightly overestimate the chloride content compared to titration. The advantage of ICP-MS is that one can express the chloride content relative to the Ca content, and thereby relative to the paste content. This is also possible with SEM-EDS. However, SEM-EDS seems to underestimate the Cl/Ca ratio compared to ICP-MS, which might be due to the preparation of the thin sections used for SEM-EDS. SEM-EDS does have the advantage that elemental profiles can be studied on a fine spatial scale (125 μm). This allowed the detection of the zone at the exposed surface with very low chloride concentrations.

- Effect of the binders:

The concretes with the different binders have relatively similar chloride profiles after 16 years of submerged exposure to sea water. Of the concretes with normal weight aggregates tested, the OPC-slag binder performs slightly better than the OPC-SF and OPC-FA binder after 16 years of exposure as it reaches the 0.07% chloride limit, associated with negligible risk of corrosion [6], at a depth of 23-29 mm whereas the other two reach that limit at 35-43 mm. The Cl/Ca ratio is higher for the OPC-FA concrete. The reason for this is unclear. One could expect that it is due to a lower Ca content, but this is not the case. Whether this is related to progressed leaching of this binder remains a question.

SEM-EDS results showed that the chloride concentration at the exposed surface is almost zero. This zone stretches a couple of 100 μm 's inwards from the exposed surface. After this zone the Cl/Ca ratio increases abruptly to a maximum at approx. 1 mm and maintains this level up to approx. 4 mm, before decreasing again moving deeper inwards from the exposed surface.

- Effect of the LWA:

The chloride profiles for the OPC-LWA concrete show higher chloride concentrations in the first 10 mm from the surface compared to the other tested concretes.

A possible explanation could be that the LWA, which is rich in aluminates and silicates, would produce pozzolanic reaction products which could bind additional chlorides. SEM-EDS maps however indicate that the LWA is not reactive.

However, when expressing the chloride content in the OPC-LWA concrete relative to the Ca content and thereby relative to the paste content, the profile is similar to the other concretes. Therefore it can be concluded that the higher paste content in the OPC-LWA concrete results in an apparent higher chloride content.

The higher paste content in the OPC-LWA concrete only seems to result in a higher chloride content near the surface relative to the concrete mass, but it does not seem to increase the ingress depth, even to the contrary.

Carbonation

- **Techniques:**
Carbonation was investigated with TGA and polarized light microscopy. TGA is performed on profile ground samples, hence the spatial resolution is limited to the resolution of grinding. Microscopy allows a better insight in the distribution of the paste carbonation. Microscopy also allows to distinguish between paste carbonation and the deposition of carbonates on the surface which cannot be done with the TGA.
- **Effect of the binders and LWA:**
The samples showed limited carbonation as the carbonation depth, determined by microscopy, did not exceed 1 mm for OPC-SF, OPC-FA and OPC-slag. This was confirmed by the TGA results for all tested concretes. The limited carbonation could be expected for concretes with such a low water:binder ratio and for submerged conditions.

Elemental changes

- **Techniques:**
The elemental changes were studied with ICP-MS and SEM-EDS. As mentioned before, the spatial resolution of the elemental changes for ICP-MS is limited to the intervals of the profile grinding as acid solubilized profile ground concrete powder is used. SEM-EDS on the other hand gives a more detailed spatial resolution (steps of 125 μm). This also brings with that ICP-MS is more representative for the half a concrete core compared to SEM-EDS which only shows the elemental changes in one track going from the surface inwards.
The elemental changes are assumed to take place in the cement paste as aggregates are assumed to be inert. Therefore the elemental changes are expressed relative to the Ca content, as the aggregates do not contain Ca and thereby Ca represents the paste. It should be noted Na and K profiles are not determined by SEM-EDS due to the low concentrations and their presence in the aggregates.
- **Effect of the binders and LWA:**
Except for the chloride content there are no considerable changes in the measured element concentrations from 10 mm and deeper inwards. Within the first 10 mm from the exposed surface, similar trends are observed for the different concretes tested.

Na: ICP-MS results show a slight enrichment in Na in the outer most section (0-1 mm). Sodium does not follow the chloride into the concrete which is in line with previous observations [8].

K: ICP-MS show a gradual decrease in the K content towards the exposed surface, indicating leaching.

Mg: ICP-MS shows an enrichment in Mg in the outer most section (0-1 mm). This can be due to the precipitation of brucite or the formation of M-S-H as observed before [8, 9]. This is confirmed by SEM-EDS which show an increase in the Mg/Ca ratio in the outermost couple of 100 μm 's.

S: ICP-MS shows a sulfur enrichment in the first two sections from the exposed surface (0-1 and 1-3 mm). SEM-EDS shows that the sulfur content near the surface is very low. It increases from 200-300 μm from the surface to reach a maximum at between 0.5 and 0.8 mm from the surface, and decreases back to the background sulfur level between 2 and 4 mm from the surface. Thus the S/Ca profile exhibits a clear peak behavior.

Cl: ICP-MS and titration indicated a lower Cl concentration at the outer most section (0-1 mm). The chloride content reaches a maximum deeper into the concrete. This is confirmed by SEM-EDS which showed very low Cl/Ca ratio's near the surface and an increase after 200-300 μm to reach a maximum at 1-4 mm from the surface. A zone of maximum Cl/Ca ratio is observed rather than a peak, which is in-line with the ICP-MS observations. The maximum chloride zone seems to be preceded by the sulfur peak. This is in-line with observations that the presence of sulfur lowers the chloride binding [10].

Portlandite: TGA indicated leaching of the Portlandite for all tested concretes. For OPC-SF and OPC-slag the leaching appeared to be limited to the first 10 mm. However, for OPC-LWA and OPC-FA the Portlandite content showed a reduction up to respectively 30 and 50 mm from the exposed surface. In the case of OPC-FA the Portlandite reduction might also be caused by consumption through the pozzolanic reaction of the fly ash

Porosity

- Techniques:
The porosity was measured by applying the PF method and by studying fluorescence impregnated thin section under a UV light in a microscope. Again both methods allow to study the porosity in a different scale: for the PF method approx. 10 mm thick discs were used whereas for the thin sections porosity can be investigated on the scale of e.g. 1 mm. The study of the thin sections indicated a densification of the paste near the surface. The micrographs were not used to quantify the porosity by image analysis as the thin sections appeared to have a varying thickness which might influence the quantification of the porosity.
- Effect of the binder:
For all tested concretes, the PF method indicated a slightly higher suction porosity towards the exposed surface which might be due to the increase paste content (wall effect). For the suction porosity in bulk (40-80 mm), the OPC-FA concrete resulted in the highest suction porosity followed by the OPC-SF concrete and the lowest suction porosity was attained by OPC-slag. This might be related to a higher degree of reaction of the slag compared to the fly ash, which thereby contributes more to a densification of the pore structure. However,

further investigation of the samples is needed in order to confirm that.

The concretes with the different binders have a similar volume of macro pores approx. 1.8 Vol.%.

- Effect of the LWA:

The volume of suction porosity of the OPC-LWA concrete is considerably higher than the suction porosity of the OPC-SF concrete. This might be partially due to the higher paste content in the OPC-LWA concrete. The macro porosity of the OPC-LWA concrete was 4 to 5 times higher than the macro porosity of the other tested concretes. This might indicate that the pores in the LWA particles are accessed during the pressurizing step of the PF method.

Moisture

- Techniques:

The degree of capillary saturation (DCS) was measured as well as the relative humidity (RH) for the approx. 10 mm thick discs. It should be noted that the discs were cut with a water cooled saw which influenced the RH measurements and to a minor extent the DCS measurements.

The RH measurements show great scatter and do not indicate any clear trend, except for the indication of self-desiccation of the split samples in the bulk.

In addition the moisture content determined on the profile ground powder prior to chloride titration is reported. One should keep in mind that the powder might have lost moisture during grinding. However, the results can be of interest to study relative differences.

- Effect of the binder:

The DCS profiles of the concrete with the different binders, show all a slight decreasing trend from the exposed surface up to approx. 30 mm, after which the DCS is fairly constant. This agrees more or less with the profiles obtained from the profile ground powder which showed a decrease up to 10-20 mm and relatively constant values deeper inwards. These results indicate self-desiccation of the concrete in the bulk.

- Effect of LWA

The DCS profile of the OPC-LWA concrete is considerably lower than the OPC-SF concrete, whereas the RH measurements are systematically higher. This could indicate that during the determination of the suction porosity by the PF method larger pores (non-capillary) were also filled. This questions the use of the PF method on such thin sections (10 mm) for an LWA concrete. The PF results obtained for the LWA concrete should be interpreted with care.

6 Conclusion

One of the aims of the study was to investigate how different binders affect chloride ingress. Surprisingly or not, the chloride profiles of the OPC-SF, OPC-slag and OPC-FA concrete appeared to be relatively similar after 16 years of submerged exposure to sea water. The critical chloride content for OPC-SF and OPC-FA concretes is however reached at slightly higher depths compared to OPC-slag. Nonetheless, one can conclude that replacing OPC with 9% SF, 20% FA + 4% SF and 30% slag +5% SF results in comparable chloride ingress after 16 years under the given conditions despite the presumed differences in composition and reactivity of these binders. A remaining question is whether the relatively low water to binder ratio and the curing prior to exposure might have overshadowed any potential difference between the tested binders.

OPC-LWA shows higher chloride concentrations near the exposed surface and a lower ingress depth compared to the other tested concretes. At first it was assumed that the LWA particles would be able to bind chlorides through a potential pozzolanic reaction thereby increasing the total chloride concentration. However, the dense sintered shell of the particles observed by SEM-EDS appeared to prevent the particles from reacting. The higher chloride concentrations can on the other hand be linked to the higher binder content of the OPC-LWA concrete when expressing the chloride profiles relative to the calcium content. Whether this higher binder content also contributes to the reduced ingress depth or whether this is related to moisture gradients, requires further research.

More in general, the chloride profiles show a maximum at 1-4 mm from the exposed surface. The lower concentration at the surface is shown to be associated with phase changes (magnesium and sulfur enrichment, leaching of calcium and potassium as well as carbonation), and not with drying and wetting cycles as often suggested in literature.

Another remarkable observation is that the centers of the concrete cores are not saturated even though the concretes have been submerged for 16 years. This might be attributed to self-desiccation and a tight pore structure due to the low water binder ratio. Whether this reduced degree of saturation in the core of the concrete is one of the determining limiting parameters for chloride ingress overshadowing the binder differences remains a question.

7 Acknowledgements

Bård Pedersen and Claus K Larsen are acknowledged for making this research project possible, for giving us access to these invaluable concrete specimens at Solsvik field station and for inviting us to assist in the core drilling. The authors also want to acknowledge Arnaud Muller, visiting PhD student from EPFL Switzerland, who assisted under the collection of the cores at Solsvik and the sampling of the cores during the following days.

8 References

1. Larsen, C.K., *Influence of concrete composition on long term chloride ingress*, in *International Conference on Bridges 2006*: Dubrovnik, Croatia.
2. Thomas, M.D.A., R.D. Hooton, A. Scott, and H. Zibara, *The effect of supplementary cementitious materials on chloride binding in hardened cement paste*. *Cement and Concrete Research*, 2012. **42**(1): p. 1-7.
3. Larsen, C., NPRA, *Concrete recipees phase 2 Solsvik*, received: 2013-03-05
4. SINTEF, *internal procedure KS 14-05-04-110 for capillary suction and porosity*, 2007.
5. Sellevold, E.J. and T. Farstad. *The PF-method - A simple way to estimate the w/c-ratio and air content of hardened concrete*. in *Proceedings ConMat'05*. 2005. Vancouver, Canada
6. Fluge, F., *Marine chlorides - A probabilistic approach to drive provisions for EN 206-1*, in *Duranet 3rd workshop - Service life design of concrete structures - from theory to standardisation2001*: Tromsø, Norway
7. Larsen, C., NPRA, *Chloride profiles after 2.5 year of exposure at the Solsvik field station* received: 2013-08-23
8. De Weerd, K., H. Justnes, and M.R. Geiker, *Changes in the phase assemblage of concrete exposed to sea water*. *Cement and Concrete Composites*, 2014. **47**(0): p. 53-63.
9. De Weerd, K. and H. Justnes, *Effect of excessive sea water on cement paste*. *Cement and Concrete Composites*, 2014. **under review - submitted 16 Jan 2014**.
10. De Weerd, K., D. Orsakova, and M.R. Geiker, *The impact of sulphate and magnesium on chloride binding in Portland cement paste*. *Cement and Concrete Research*, 2014. **Under review - Submitted 14 April 2014**.

Appendix

Tabulated data 1: Chloride profiles 2
Tabulated data 2: Moisture content profile ground powder 2
Tabulated data 3: ICP-MS 3
Tabulated data 4: TGA 4
Tabulated data 5: SEM-EDS Part 1 of 2. 5
Tabulated data 6: SEM-EDS Part 2 of 2. 6
Tabulated data 7: PF results 7
Tabulated data 8: Relative humidity 8

Tabulated data 1: Chloride profiles

depth [mm]	Cl 16y NTNU [% dry concrete mass]			
	OPC-SF	OPC-slag	OPC-FA	OPC-LWA
0.5	0.40	0.36	0.72	0.60
2	0.67	0.61	0.83	0.84
4	0.57	0.54	0.69	0.76
6	0.52	0.50	0.52	0.73
8	0.43	0.45	0.51	0.69
11	0.41	0.31	0.46	0.62
15	0.33	0.22	0.33	0.50
20	0.24	0.19	0.33	0.32
26	0.20	0.10	0.20	0.13
32	0.12	0.06	0.11	0.02
39	0.08	0.05	0.03	0.04
47	0.04	0.04	0.04	0.02
55	0.04	0.00	0.04	0.03
63	0.04	0.00	0.03	0.02
71	0.04	0.00	0.04	0.03
79	0.04	0.03	0.02	0.02
87	0.03	0.02	0.05	0.05

Tabulated data 2: Moisture content profile ground powder

depth [mm]	moisture content 16y NTNU [%]			
	OPC-SF	OPC-slag	OPC-FA*	OPC-LWA
0.5	5.68	4.19	2.67	4.27
2	4.62	3.08	3.17	3.45
4	3.85	2.50	1.67	2.89
6	3.07	3.26	0.38	2.91
8	2.31	2.50	1.54	2.71
11	3.07	2.11	1.53	2.30
15	2.49	1.73	2.50	2.30
20	2.31	1.54	2.13	2.50
26	2.30	1.54	1.31	2.68
32	1.73	1.54	1.73	2.69
39	2.11	1.73	1.54	2.50
47	2.12	1.35	1.92	2.50
55	1.93	1.73	1.74	2.69
63	1.54	1.54	2.30	2.69
71	1.73	0.96	2.33	2.50
79	1.92	1.73	2.34	2.49
87	1.35	0.96	2.12	2.87

Tabulated data 3: ICP-MS

	depth [mm]	Na	Mg	Al	Si	S	Cl	K	Ca	Fe
		[mol/g concrete]								
OPC-SF	0.5	6.8E-5	3.1E-4	2.4E-4	8.6E-4	1.3E-4	1.1E-4	3.5E-5	3.8E-3	1.3E-4
	2	3.0E-5	1.2E-4	2.3E-4	6.0E-4	1.0E-4	2.1E-4	4.6E-5	2.2E-3	1.2E-4
	4	2.8E-5	1.0E-4	2.0E-4	6.0E-4	6.9E-5	1.8E-4	5.1E-5	1.9E-3	1.1E-4
	6	3.2E-5	1.1E-4	2.3E-4	5.8E-4	6.5E-5	1.6E-4	6.1E-5	1.9E-3	1.3E-4
	8	3.5E-5	9.1E-5	2.1E-4	6.2E-4	6.2E-5	1.4E-4	5.9E-5	1.7E-3	1.1E-4
	8	3.2E-5	9.0E-5	2.1E-4	6.0E-4	5.9E-5	1.3E-4	5.8E-5	1.7E-3	1.1E-4
	15	3.4E-5	9.4E-5	2.1E-4	5.7E-4	5.9E-5	9.8E-5	6.4E-5	1.7E-3	1.1E-4
	32	3.8E-5	8.1E-5	1.8E-4	4.6E-4	4.6E-5	3.5E-5	6.6E-5	1.4E-3	9.5E-5
79	4.1E-5	8.7E-5	2.2E-4	6.5E-4	5.1E-5	2.6E-6	7.0E-5	1.5E-3	1.2E-4	
OPC-slag	0.5	5.3E-5	3.9E-4	3.6E-4	3.9E-4	1.1E-4	1.1E-4	4.6E-5	2.8E-3	9.1E-5
	2	2.6E-5	1.9E-4	3.0E-4	5.9E-4	7.3E-5	1.8E-4	5.0E-5	1.8E-3	8.4E-5
	2	2.7E-5	1.8E-4	2.8E-4	5.7E-4	6.8E-5	1.7E-4	5.2E-5	1.6E-3	8.4E-5
	4	3.1E-5	1.8E-4	2.9E-4	5.7E-4	5.9E-5	1.6E-4	6.4E-5	1.6E-3	9.5E-5
	6	3.0E-5	1.7E-4	2.9E-4	5.9E-4	5.7E-5	1.5E-4	5.6E-5	1.6E-3	8.5E-5
	8	3.2E-5	1.6E-4	2.7E-4	5.4E-4	5.8E-5	1.3E-4	5.5E-5	1.6E-3	8.2E-5
	15	3.9E-5	1.4E-4	2.7E-4	5.6E-4	4.8E-5	6.9E-5	6.4E-5	1.3E-3	9.0E-5
	32	3.4E-5	1.6E-4	2.4E-4	5.5E-4	5.0E-5	1.9E-5	5.7E-5	1.4E-3	1.0E-4
79	3.8E-5	1.5E-4	2.6E-4	5.1E-4	4.1E-5	1.7E-6	6.9E-5	1.2E-3	8.7E-5	
OPC-FA	0.5	5.7E-5	3.3E-4	3.1E-4	3.4E-4	1.3E-4	2.2E-4	4.9E-5	2.5E-3	1.3E-4
	2	3.9E-5	1.6E-4	2.8E-4	6.9E-4	1.1E-4	2.5E-4	5.6E-5	1.8E-3	1.1E-4
	4	3.6E-5	1.1E-4	2.7E-4	6.1E-4	5.9E-5	2.0E-4	7.8E-5	1.4E-3	1.1E-4
	6	3.4E-5	8.7E-5	2.3E-4	4.9E-4	4.0E-5	1.5E-4	7.3E-5	1.0E-3	1.0E-4
	8	3.5E-5	9.6E-5	2.4E-4	5.9E-4	4.2E-5	1.6E-4	7.6E-5	1.2E-3	1.1E-4
	15	3.1E-5	8.1E-5	1.9E-4	5.0E-4	3.9E-5	9.8E-5	5.5E-5	1.2E-3	9.1E-5
	32	4.2E-5	8.4E-5	2.1E-4	5.9E-4	4.9E-5	3.0E-5	6.7E-5	1.3E-3	1.1E-4
	79	4.9E-5	9.6E-5	2.6E-4	7.2E-4	6.5E-5	2.2E-6	6.5E-5	1.8E-3	1.2E-4
OPC-LWA	0.5	8.7E-5	2.6E-4	2.4E-4	7.0E-4	1.2E-4	1.6E-4	3.3E-5	4.2E-3	1.3E-4
	2	4.6E-5	1.4E-4	3.0E-4	7.9E-4	1.1E-4	2.6E-4	4.3E-5	2.8E-3	1.5E-4
	4	5.1E-5	1.2E-4	2.9E-4	8.4E-4	9.1E-5	2.6E-4	4.5E-5	2.5E-3	1.4E-4
	6	5.2E-5	9.8E-5	2.5E-4	7.2E-4	7.9E-5	2.4E-4	4.1E-5	2.3E-3	1.2E-4
	8	4.9E-5	1.1E-4	2.7E-4	7.5E-4	8.2E-5	2.4E-4	4.1E-5	2.5E-3	1.2E-4
	15	5.3E-5	9.4E-5	2.5E-4	7.2E-4	7.9E-5	1.6E-4	4.3E-5	2.2E-3	1.2E-4
	32	5.0E-5	9.8E-5	2.3E-4	7.7E-4	7.9E-5	4.5E-6	4.8E-5	2.4E-3	1.1E-4
	79	5.4E-5	9.8E-5	2.3E-4	8.0E-4	8.1E-5	3.3E-6	4.6E-5	2.6E-3	1.2E-4

Tabulated data 4: TGA

	depth [mm]	CH	H40-450C [% of mass at 850C]	CaCO3
OPC-SF	0.5	0.77	11.00	24.14
	2	1.22	8.04	4.31
	4	1.32	6.63	3.26
	6	1.25	5.59	2.97
	8	1.31	5.04	2.70
	11	1.58	5.53	2.95
	15	1.60	5.00	2.65
	20	1.58	4.75	2.49
	26	1.71	4.63	2.25
	71	1.85	3.54	0.91
OPC-slag	0.5	0.29	6.42	11.03
	2	0.80	5.92	3.42
	4	0.98	5.00	2.38
	6	1.12	5.08	2.43
	8	1.35	5.54	2.39
	15	1.16	3.76	1.46
	20	1.33	3.84	1.26
	26	1.49	3.75	0.97
	71	1.14	3.01	0.82
	79	1.29	3.28	0.82
OPC-FA	0.5	0.00	7.33	9.35
	2	0.00	6.20	3.17
	4	0.00	4.24	1.76
	6	0.00	3.21	1.42
	8	0.27	3.51	1.47
	15	0.30	3.38	1.52
	20	0.59	4.19	1.56
	26	0.70	3.62	1.25
	32	0.82	3.38	1.16
	39	1.02	3.73	1.18
	47	0.90	3.18	0.98
	79	1.48	4.66	2.15
87	1.47	4.60	1.52	
OPC-LWA	0.5	0.89	7.33	23.60
	2	1.02	5.76	4.65
	4	1.26	5.44	3.96
	6	1.26	4.72	1.94
	8	1.81	5.76	2.07
	15	2.16	5.42	1.87
	26	2.71	5.78	1.70
	47	2.61	5.76	1.80
71	2.99	5.74	1.59	
79	3.01	5.90	1.76	

Tabulated data 5: SEM-EDS Part 1 of 2.

	depth [mm]	Cl/Ca	S/Ca molar ratio	Mg/Ca
OPC-SF_1	0.07	0.005	0.008	0.092
	0.15	0.003	0.009	0.124
	0.30	0.005	0.031	0.045
	0.57	0.034	0.052	0.042
	1.09	0.063	0.046	0.036
	1.49	0.054	0.034	0.035
	2.02	0.067	0.031	0.037
	2.91	0.065	0.035	0.041
	3.91	0.063	0.032	0.042
	5.02	0.067	0.037	0.039
	10.13	0.050	0.031	0.093
	20.01	0.036	0.033	0.037
	29.97	0.025	0.031	0.042
	39.33	0.014	0.030	0.031
OPC-SF_2	0.05	0.004	0.009	0.245
	0.14	0.004	0.013	0.088
	0.30	0.023	0.041	0.043
	0.58	0.046	0.053	0.043
	1.03	0.056	0.039	0.045
	1.50	0.048	0.031	0.044
	2.03	0.058	0.032	0.039
	3.17	0.054	0.030	0.045
	4.00	0.053	0.031	0.034
	5.00	0.047	0.032	0.039
	9.96	0.036	0.034	0.037
	20.29	0.034	0.029	0.047
	20.34	0.031	0.031	0.041
	30.13	0.019	0.029	0.044
40.15	0.011	0.034	0.000	
OPC-slag	0.07	0.016	0.019	0.519
	0.17	0.013	0.010	0.392
	0.29	0.008	0.009	0.263
	0.60	0.027	0.079	0.104
	0.99	0.057	0.052	0.090
	1.88	0.083	0.037	0.140
	2.97	0.076	0.038	0.101
	3.95	0.074	0.034	0.090
	4.97	0.069	0.036	0.088
	9.99	0.045	0.032	0.087
	19.97	0.019	0.035	0.099
	30.04	0.010	0.038	0.090
	40.10	0.004	0.033	0.120

Tabulated data 6: SEM-EDS Part 2 of 2.

	depth [mm]	Cl/Ca	S/Ca molar ratio	Mg/Ca
OPC-FA_1	0.07	0.008	0.011	0.112
	0.16	0.014	0.022	0.105
	0.32	0.048	0.067	0.054
	0.59	0.070	0.052	0.053
	1.00	0.092	0.037	0.050
	1.50	0.087	0.035	0.050
	1.98	0.089	0.034	0.057
	2.99	0.083	0.034	0.041
	4.00	0.084	0.033	0.045
	5.00	0.076	0.040	0.048
	10.02	0.067	0.033	0.043
	19.98	0.036	0.032	0.040
	30.01	0.020	0.032	0.061
	39.95	0.008	0.032	0.043
OPC-FA_2	0.06	0.010	0.012	0.518
	0.17	0.006	0.016	0.141
	0.31	0.036	0.061	0.044
	0.60	0.062	0.073	0.039
	1.02	0.084	0.047	0.049
	2.00	0.079	0.040	0.045
	2.99	0.096	0.034	0.050
	4.01	0.087	0.031	0.040
	5.00	0.085	0.034	0.049
	9.99	0.061	0.030	0.041
	20.13	0.035	0.035	0.046
	29.89	0.019	0.038	0.040
	39.91	0.006	0.029	0.050
	OPC-LWA	0.06	0.007	0.026
0.14		0.007	0.022	0.125
0.29		0.014	0.005	0.043
0.45		0.059	0.066	0.038
0.61		0.071	0.052	0.080
1.03		0.083	0.037	0.031
1.60		0.091	0.032	0.041
2.02		0.088	0.028	0.037
2.93		0.097	0.030	0.034
4.03		0.078	0.028	0.036
5.00		0.072	0.029	0.040
10.00		0.069	0.029	0.040
18.92		0.037	0.028	0.039
32.67		0.002	0.035	0.038
32.74		0.000	0.033	0.051
42.40	0.000	0.030	0.039	

Tabulated data 7: PF results

	depth [mm]	Suc por 50C	Suc por 105C [Vol%]	DCS	Macro pores
OPC-SF	9.8	10.79	13.73	97.69	1.69
	20.9	10.87	13.60	97.28	1.74
	44.6	11.08	13.79	96.39	1.59
	55.45	11.15	13.84	97.14	1.31
	66.65	10.84	13.38	95.00	1.30
	78.05	10.94	13.49	96.12	1.39
	splitt	10.50	13.18	95.01	1.27
	splitt	10.70	13.53	95.26	1.02
OPC-slag	7.7	11.74	14.71	97.47	1.40
	19.8	11.06	13.35	95.23	1.51
	32.05	10.82	12.99	94.13	1.47
	43.6	10.53	12.62	94.77	1.34
	54.85	10.96	13.18	94.30	1.43
	67.1	10.54	12.64	94.30	1.54
	73.6	10.20	12.22	94.29	1.60
	splitt	10.58	12.75	92.22	0.89
OPC-FA	9.75	12.37	15.25	97.91	1.23
	21.7	12.21	14.92	95.60	1.19
	33.25	11.51	14.06	93.83	1.24
	33.25	11.60	14.11	93.05	1.33
	44.45	11.80	14.33	93.00	1.41
	68.6	11.61	14.09	93.29	1.24
	80.85	11.89	14.44	93.33	1.24
	splitt	11.79	14.44	92.19	1.26
OPC-LWA	8.55	14.80	17.68	94.67	11.28
	20.5	14.87	17.78	88.81	8.86
	32.1	13.65	16.69	88.63	8.09
	44.55	13.84	16.78	88.27	8.28
	56.4	14.23	17.28	90.92	8.29
	68.3	14.45	17.46	91.01	8.49
	80	14.30	17.34	92.36	7.65
	splitt	14.01	17.11	85.63	7.73

Tabulated data 8: Relative humidity

	depth [mm]	RH [%]
OPC-SF	8.15	96.8
	19.35	90.8
	30.4	90.4
	41.85	90.7
	53.9	92.4
	65.25	95.2
	75.95	93.3
	split	88.1
OPC-slag	10.2	91.6
	21	93.2
	33.4	94.7
	43.85	94.8
	54.1	94.5
	64.1	96.4
	73.6	93.4
	split	91.5
	split	89.9
OPC-FA	8.95	93.3
	19.85	93.2
	31.15	93.2
	43.3	95.5
	55.55	90.8
	66.7	94.6
	77.35	96.8
	split	91.3
	split	92.5
OPC-LWA	10.9	96.8
	22.9	97.6
	34.55	95.2
	46.7	98.6
	58.3	96.4
	70.1	98.0
	82.4	98.3
	split	95.5



Statens vegvesen
Vegdirektoratet
Publikasjonsekspedisjonen
Postboks 8142 Dep 0033 OSLO
Tlf: (+47 915) 02030
publvd@vegvesen.no

ISSN: 1893-1162

vegvesen.no

Trygt fram sammen